Generalized van der Waals theory for the twist elastic modulus and helical pitch of cholesterics

H. H. Wensink* and G. Jackson

Department of Chemical Engineering, Imperial College London,
South Kensington Campus, London SW7 2AZ, United Kingdom
(Dated: May 26, 2009)

We present a generalized van der Waals theory for a lyotropic cholesteric system of chiral spherocylinders based on the classical Onsager theory for hard anisometric bodies. The rods consist of a hard spherocylindrical backbone surrounded with a square-well potential to account for attractive (or soft repulsive) interactions. Long-ranged chiral interactions are described by means of a simple pseudo-scalar potential which is appropriate for weak chiral forces of a predominant electrostatic origin. Based on the formalism proposed by Straley [Phys. Rev. A **14**, 1835 (1976)] we derive explicit algebraic expressions for the twist elastic modulus and the cholesteric pitch for rods as a function of density and temperature. The pitch varies non-monotonically with density, with a sharp decrease at low packing fractions and a marked increase at higher packing fractions. A similar trend is found for the temperature dependence. The unwinding of the helical pitch at high densities (or low temperatures) originates from a marked increase in the local nematic order and a steep increase of the twist elastic resistance associated with near-parallel local rod configurations. This contrasts with the commonly held view that the increase in pitch with decreasing temperature as often observed in cholesterics is due to layer formation resulting from pre-smectic fluctuations. The increase in pitch with increasing temperature is consistent with an entropic unwinding as the chiral interaction becomes less and less significant than the thermal energy. The variation of the pitch with density, temperature and contour length is in qualitative agreement with recent experimental results on colloidal *fd* rods.

PACS numbers: 83.80.Xz, 61.30.Cz, 82.70.Dd

I.   INTRODUCTION

Cholesteric liquid crystals (LCs) display a variety of extraordinary features due to the existence of a mesoscopic helical structure which is best known for its exceptionally large optical rotational power employed in LC display technology. In contrast to a common nematic phase, where the nematic director is homogeneous throughout the system, the cholesteric (chiral nematic) phase is characterized by a helical arrangement of the director field along a common pitch axis. As a result, the cholesteric phase possesses an additional mesoscopic length scale, commonly referred to as the 'pitch length', which characterizes the distance along the pitch axis over which the local director makes a full revolution[1].

Derivatives of cholesterol, chiral molecules which were the first mesogenic substances to be recognized in studies of the melting point and optical properties of carrot extracts by Reinitzer[2] and Lehmann[3], belong to the thermotropic class of liquid crystals where phase transitions are brought about by a variation in the temperature; a large number of thermotropic mesogens with a low to moderate molecular weight that form chiral nematic phases have now been isolated or synthesized. Their widespread use in optoelectronic applications (e.g., twisted nematic liquid crystal displays in laptop computers, televisions, and mobile phones) is a direct consequence of the unique rheological, electrical and optical properties imparted by the chiral structures.

Lyotropic chiral systems, involving high molecular-weight particles in solution where the ordering behavior is primarily governed by the solute concentration, are also common. Examples are bio-colloidal systems such as DNA[4,5] and the rod-like *fd*-virus[6], stiff polymers such as polypeptides[7,8], polysaccharides[9] or cellulose derivatives[10], and chiral micelles[11]. In these systems, the cholesteric pitch is very sensitive to concentration, temperature as well as the solvent conditions such as ionic strength and pH. The dependence of the pitch upon these variables has been the subject of intense experimental research (see for example references[4,12,13,14,15,16,17,18,19,20,21,22]).

Theoretical attempts to predict the behavior of the cholesteric pitch are challenging owing to the complexity of the underlying chiral interaction[23] and the inhomogeneous and anisotropic nature of the phase. Course-grained model potentials aimed at capturing the essentials of the complex molecular nature of the electrostatics of the surface of such macromolecules have been devised mainly for DNA[24,25,26,27,28]. A more general electrostatic model potential for chiral interactions was proposed much earlier by Goossens[29] based on a spatial arrangement of dipole-dipole and dipole-quadrupole interactions which can be cast into a multipole expansion in terms of tractable pseudo-scalar potentials[30]. This type of electrostatic description of the chiral interaction can be combined with a Maier-Saupe mean-field treatment (see, for example references[31,32,33,34,35,36], or with a bare hard-core model and treated within the seminal theory of Onsager[37] (as in the recent study of chiral hard spherocylinders for systems with perfect local nematic order[38]).

Taking the alternative view of a steric origin for the chiral interactions, Straley[39] combined a leading order pseudo-scalar form with a hard rod model to create a basic chiral model (hard threaded rod) for lyotropic cholesterics. Though influenced by the work of Goossens on electrostatic forces, the potential used by Straley is appropriate for short-ranged steric chiral interactions mediated by a thin helical thread enveloping each rod. By extending the theory of Onsager[37] to systems with non-uniform director fields, microscopic expressions for the macroscopic twist energy associated with a bulk cholesteric structure can be deduced. The theoretical treatment was later elaborated in a paper by Odijk[40] leading to microscopic scaling expressions for the twist elastic constant and helical pitch of both rigid and semi-flexible rods. Similar relations, albeit with different scaling exponents, were obtained by Pelcovits[41] based on a corkscrew model.

At this stage one should also acknowledge the related studies on the link between the orientational order parameters and the elastic constants in nematics, which have been influential in shaping some of the theories of chiral phases. A mean-field treatment of particles with electrostatic chirality but no shape anisotropy has been developed[42,43,44], as have Onsager DFT theories for anisotropic hard rod-like particles[45,46,47,48] and hard rods with attractive mean-fields[49,50], the latter being closely related to the achiral contribution of the model employed in our study. The principal finding of this body of work is that the elastic constants are predicted to be proportional to the square of the nematic order parameter, at least for system with weak orientational order, confirming experimental observation[51] and the results of molecular simulation[52]. Such a treatment has also been extended to a description of the elastic constants in smectic phases[53,54].

The underlying microscopic physical feature (steric or electrostatic) responsible for the formation of chiral nematic phases is still a matter of debate and controversy. In has been known for some time that the nature of the solvent can have a dramatic effect on the pitch of cholesteric phases, and can even reverse the sense of the twist (e.g., see the study of Robinson[4] on poly-γ-L-benzyl-L-glutamate PBLG, a synthetic polypeptide with an α helical conformation, in achiral solvents such as dioxane and dichloromethane), hinting to a solvent effect of electrostatic origin. In a beautifully revealing but rather overlooked paper, Coates and Gray[55] showed that the replacement of a hydrogen by a deuterium atom on the carbon backbone of an originally achiral thermotropic mesogen is sufficient to induce a cholesteric structure; the carbon-hydrogen and carbon-deuterium bond lengths are both 1.085 Å so one would expect the "steric shape" of both molecules to be very similar, indicating that in this case at least the chirality is of a weak and subtle electrostatic nature.

The fact that the pitch of the cholesteric phase in aqueous solutions of the filamentous fd virus is very sensitive to the ionic strength of the medium but still persists after coating the virus with polyethylene oxide polymer (which would mask any short-range chirality in the particle shape) is also indicative of an electrostatic origin to the interparticle chiral interaction in such lyotropic systems[16,56]. This lends credence to the use of electrostatic interactions of the type proposed by Goossens[29] decorated with an achiral non-spherical core as physically reasonable microscopic models for chiral systems; an additional repulsive steric chiral core could of course also be incorporated in a more realistic treatment (e.g., see reference[57]), but this is beyond the scope of our work.

The helical pitch of cholesteric thermotropic mesogens is almost invariably found to be a decreasing function of temperature[1], which is commonly attributed to the presence of an underlying smectic-A phase at lower temperatures: a twisted chiral structure is incommensurate with the smectic layering leading to an unwinding of the pitch as one approaches the transition[58,59]. What is surprising is that this thermally induced decrease in the pitch can occur over many decades in temperature, where one would not expect effects due to pretransitional smectic order. An increase in pitch with increasing temperature has been reported for the cholesterol ester, cholesteryl [2-(2-ethoxyethoxy-ethyl] carbonate (CEEC)[60]; interestingly in the case of CEEC the transition from the isotropic phase to the chiral nematic does not appears to be followed by a transition to a smectic phase with a further decrease in temperature, but rather to the formation of a crystalline state[61]. A remarkable sense inversion in the helical pitch with temperature has also been found in thermotropic (solvent free) polypeptides[62] and cellulose derivatives[63], and in mixtures of right-handed cholesterol chloride and left-handed cholesterol myristate[64], indicating a subtle balance in the forces giving rise to chiral phases.

The situation is just as intriguing in the case of lyotropic systems where depending on the range of temperature, both negative and positive slopes of the pitch can be observed. At relatively high temperatures a marked increase of the pitch has been found in polypeptide systems (mixtures of PBLG in dioxane, chloroform, and dichloromethane)[17] and in aqueous solutions of fd-virus rods[15]. In the latter system the pitch is found to increase with increasing concentration well before the transition to a smectic phase. An unwinding of the cholesteric phase (with a corresponding increase in the pitch) is also observed in aqueous solutions of DNA[12] as the concentration of the macromolecules is increased towards a high-density hexagonal columnar (positionally ordered) state[65]; this is analogous to the divergence of the pitch found in thermotropic mesogens as one approaches the smectic state on lowering the temperature.

The early molecular-field approaches based on the Maier-Saupe electrostatic picture of the mesogenic interaction[31,32] fail to give a consistent picture of the variation of the pitch with temperature for cholesteric phases, mainly because of the lack of a hard-core exclude

volume contribution in the interaction which plays an essential role in the stabilization of the orientationally ordered phase[37].

The important role of the mesogen's shape in understanding the temperature dependence of the pitch was pointed out early on by Kimura *et al.*[66]. The insensitivity of the pitch to temperature found in lattice simulations of sites interacting through a Goossens electrostatic potential[67] supports the view that one requires a balance between the opposing twist elastic forces (which are primarily a consequence of the repulsive interactions) and the chiral torque (due to the cholesteric interactions) to observe the subtle dependencies found for the pitch. A proper account of the rod-like backbone turns out to be essential to explain the unwinding of the cholesteric structure with increasing temperature[22,38].

It is clear from the preceding discussion that a number of important questions remain unresolved in our understanding of the origin of chirality and the related dependence of the helical pitch on the thermodynamic variables such as temperature and composition. Does one require the presence of an underlying smectic (or columnar) phase to observe an increase in pitch with decreasing temperature? Under what conditions would one expect a thermally induced unwinding of the chiral nematic phase and when would a non-monotonic temperature dependence of the pitch be obtained? What are the competing roles of repulsive excluded volume interactions, and isotropic and anisotropic (chiral and achiral) attractive interactions in stabilizing a twisted equilibrium structure? As de Gennes and Prost state in their monograph when referring to the temperature dependence of the pitch: "Their origin is not yet quite clear". In this paper, we will build upon the idea of coupling a hard core with chiral electrostatic interactions and present a microscopic theory for rigid chiral spherocylinders of arbitrary aspect ratio.

Our motivation for the analysis is three-fold. First of all, most investigations thus far have been restricted to infinitely thin rod-like species. We show that the rod thickness plays a crucial role in the behavior of the pitch in cholesteric systems with strong orientational order and helps to account for a non-monotonic dependence of the pitch with temperature and concentration. Secondly, the role of long-range chiral and achiral dispersive forces are investigated here by means of a simple square-well (SW) potential. This allows us to probe the generic temperature dependence of the pitch for chiral rods where additional achiral attractions (or soft-repulsions) are at play. Finally, we pay particular attention to the implications of chirality in the inter-particle interactions on the phase behavior. Our results are entirely algebraic and contain explicit expressions for the twist energy, elastic modulus, and cholesteric pitch as a function of density and temperature for a given rod aspect-ratio and set of intermolecular SW parameters such as the interaction range and the relative magnitude of the chiral and achiral attractive/soft-repulsive rod interactions. The results

are fully consistent with experimental results for fd-virus rods and may prove helpful in interpreting observations in other cholesteric systems.

This paper is laid out as follows. We start with a brief exposition of Straley's theory for the deformation free energy of the cholesteric state in Sec. II. A suitable spherocylinder potential is introduced in Sec. III and incorporated into the deformation free energy through a van der Waals treatment based on the Onsager-Parsons theory for anisometric hard bodies. In Sec. IV, microscopic expressions for the twist parameters and cholesteric pitch is derived. These are analyzed and the predictions compared with experimental results in Sec V. Finally, some concluding remarks are made in Sec. VI. Technical issues will be relegated to a number of Appendices.

II. MICROSCOPIC THEORY FOR THE TWISTED NEMATIC

To describe the properties of the cholesteric phase we will follow closely the analysis proposed by Straley[39,68]. The aim is to calculate the distortion free energy associated with non-uniform nematic director fields. In a distorted (e.g., twisted) nematic phase the director is no longer spatially uniform but depends on position. The same holds for the orientational distribution function (ODF), $f(\hat{\mathbf{u}} \cdot \hat{\mathbf{n}}(\mathbf{r}))$ which describes the probability of finding a particle with a given orientational unit vector $\hat{\mathbf{u}}$ with respect to a locally varying director $\hat{\mathbf{n}}(\mathbf{r})$. Within an Onsager-type formulation[37], the excess Helmholtz free energy of a distorted nematic state of N particles in a volume V can be cast in the following form:

$$F^{\text{ex}} = \frac{\rho^2}{2} \int d\mathbf{s}\Phi(\mathbf{r}_{12}; \hat{\mathbf{u}}_1, \hat{\mathbf{u}}_2) f(\hat{\mathbf{u}}_1 \cdot \hat{\mathbf{n}}(\mathbf{r}_1)) f(\hat{\mathbf{u}}_2 \cdot \hat{\mathbf{n}}(\mathbf{r}_2)),$$
(1)

with $\int d\mathbf{s} = \iiint d\mathbf{r}_1 d\mathbf{r}_2 d\hat{\mathbf{u}}_1 d\hat{\mathbf{u}}_2$ and $\rho = N/V$ the number density. The kernel Φ accounts for the pair interaction of two rods for a relative centre-of-mass separation $\mathbf{r}_{12} = \mathbf{r}_2 - \mathbf{r}_1$ and orientations $\hat{\mathbf{u}}_1$, $\hat{\mathbf{u}}_2$. This quantity will be fully specified later. Note that, strictly, $f = 1/4\pi$ in the isotropic state where the particle orientations are completely random and the director field becomes irrelevant.

If the spatial variation of the local nematic director is weak such that the associated distortion wavelength is much larger than the particle dimensions, the ODF may be approximated by a Taylor expansion. For the spatial integration it is expedient to switch to a new coordinate system, $\mathbf{r}_i \to \mathbf{R} \pm \mathbf{r}_{12}/2$ for $i = 1, 2$, in terms of $\mathbf{R} = (\mathbf{r}_1 + \mathbf{r}_2)/2$ and the centre-of mass distance $\mathbf{r}_{12}$. Expanding the ODF then gives

$$f(\hat{\mathbf{u}}_i \cdot \hat{\mathbf{n}}(\mathbf{r}_i)) = f(\hat{\mathbf{u}}_i \cdot \hat{\mathbf{n}}(\mathbf{R})) \pm \frac{\mathbf{r}_{12} \cdot \nabla}{2} f(\hat{\mathbf{u}}_i \cdot \hat{\mathbf{n}}(\mathbf{R})) + \mathcal{O}\left[(\nabla \cdot \mathbf{r}_{12})^2\right].$$
(2)

With this result, the excess free energy for weak director

gradients becomes after some rearrangement

$$
\begin{aligned}
F^{\text{ex}} &= \frac{\rho^2}{2} \int d\mathbf{s}' \Phi(\mathbf{r}_{12}; \hat{\mathbf{u}}_1, \hat{\mathbf{u}}_2) f(\hat{\mathbf{u}}_1 \cdot \hat{\mathbf{n}}(\mathbf{R})) f(\hat{\mathbf{u}}_2 \cdot \hat{\mathbf{n}}(\mathbf{R})) \\
&+ \frac{\rho^2}{2} \int d\mathbf{s}' \Phi(\mathbf{r}_{12}; \hat{\mathbf{u}}_1, \hat{\mathbf{u}}_2) f(\hat{\mathbf{u}}_1 \cdot \hat{\mathbf{n}}(\mathbf{R})) \dot{f}(\hat{\mathbf{u}}_2 \cdot \hat{\mathbf{n}}(\mathbf{R})) \\
&\times [(\mathbf{r}_{12} \cdot \nabla)\hat{\mathbf{n}}(\mathbf{R}) \cdot \hat{\mathbf{u}}_2] \\
&- \frac{\rho^2}{4} \int d\mathbf{s}' \Phi(\mathbf{r}_{12}; \hat{\mathbf{u}}_1, \hat{\mathbf{u}}_2) \dot{f}(\hat{\mathbf{u}}_1 \cdot \hat{\mathbf{n}}(\mathbf{R})) \dot{f}(\hat{\mathbf{u}}_2 \cdot \hat{\mathbf{n}}(\mathbf{R})) \\
&\times [(\mathbf{r}_{12} \cdot \nabla)\hat{\mathbf{n}}(\mathbf{R}) \cdot \hat{\mathbf{u}}_1][(\mathbf{r}_{12} \cdot \nabla)\hat{\mathbf{n}}(\mathbf{R}) \cdot \hat{\mathbf{u}}_2] \\
&+ \cdots,
\end{aligned} \tag{3}
$$

with $\int d\mathbf{s}' = \iiint d\mathbf{R} d\mathbf{r}_{12} d\hat{\mathbf{u}}_1 d\hat{\mathbf{u}}_2$ and $\dot{f} = \partial f(\hat{\mathbf{u}}_i \cdot \hat{\mathbf{n}}(\mathbf{R}))/\partial(\hat{\mathbf{u}}_i \cdot \hat{\mathbf{n}}(\mathbf{R}))$. Let us now consider a twist deformation of the director with a helix axis along the z-direction of the laboratory frame. Assuming the local nematic director to describe a perfect helix, we can parametrize the director field as follows

$$
\hat{\mathbf{n}}(\mathbf{R}) = \cos(qZ)\hat{\mathbf{x}} + \sin(qZ)\hat{\mathbf{y}}, \tag{4}
$$

with $q = 2\pi/p$ the magnitude of the pitch wave vector and p the length of the cholesteric pitch. For small wave vectors, $qa \ll 1$ (with a the typical range of the pair potential) the trigonometric functions can be expanded to leading order and the spatial dependence of the director approximated as

$$
\hat{\mathbf{n}}(\mathbf{R}) = \hat{\mathbf{x}} + qZ\hat{\mathbf{y}} + \mathcal{O}(q^2). \tag{5}
$$

The free energy density of the twisted nematic state can then be expressed as

$$
\begin{aligned}
\frac{F^{\text{ex}}}{V} &= \frac{\rho^2}{2} \iint d\hat{\mathbf{u}}_1 d\hat{\mathbf{u}}_2 M_0(\hat{\mathbf{u}}_1, \hat{\mathbf{u}}_2) f(\hat{\mathbf{u}}_1) f(\hat{\mathbf{u}}_2) \\
&- K_t q + \frac{1}{2} K_2 q^2,
\end{aligned} \tag{6}
$$

where the coefficients pertain to the twist energy and twist elastic contributions, respectively:

$$
\begin{aligned}
K_t(\hat{\mathbf{n}} \cdot \nabla \times \hat{\mathbf{n}}) &= -\frac{\rho^2}{2} \iint d\hat{\mathbf{u}}_1 d\hat{\mathbf{u}}_2 M_1(\hat{\mathbf{u}}_1, \hat{\mathbf{u}}_2) \\
&\times u_{2y} f(\hat{\mathbf{u}}_1) \dot{f}(\hat{\mathbf{u}}_2)
\end{aligned} \tag{7}
$$

$$
\begin{aligned}
K_2(\hat{\mathbf{n}} \cdot \nabla \times \hat{\mathbf{n}})^2 &= -\frac{\rho^2}{2} \iint d\hat{\mathbf{u}}_1 d\hat{\mathbf{u}}_2 M_2(\hat{\mathbf{u}}_1, \hat{\mathbf{u}}_2) \\
&\times u_{1y} u_{2y} \dot{f}(\hat{\mathbf{u}}_1) \dot{f}(\hat{\mathbf{u}}_2).
\end{aligned} \tag{8}
$$

The first contribution, (Eq. (7)), is non-vanishing only if the rod interactions are chiral, as we will see later on. It provides a measure for the torque-field exerted by the microscopic chiral interaction which favors the twist distortion. The second term, Eq. (8), provides a microscopic expression for the twist elastic modulus K_2 of the Frank elastic free energy[69]. The elastic contribution is a restoring (Hookian) term in the free energy which resists the

twist deformation. The quantities $M_i(\hat{\mathbf{u}}_1, \hat{\mathbf{u}}_2)$ are given by the following *moment* spatial integrals over the interaction kernel Φ:

$$
M_k(\hat{\mathbf{u}}_1, \hat{\mathbf{u}}_2) = \int d\mathbf{r}_{12} \Phi(\mathbf{r}_{12}; \hat{\mathbf{u}}_1, \hat{\mathbf{u}}_2) z_{12}^k, \quad (k = 0, 1, 2). \tag{9}
$$

In case of achiral hard particles, only the reference term in Eq. (6) needs to be considered. Moreover, with $M_0(\hat{\mathbf{u}}_1, \hat{\mathbf{u}}_2) = v_{\text{excl}}(\hat{\mathbf{u}}_1, \hat{\mathbf{u}}_2)$, the excluded volume of a pair of particles, the original Onsager free energy[37] is recovered as required.

For chiral nematic systems the equilibrium value of the cholesteric pitch is found by balancing the chiral forces inducing the twist deformation with the elastic forces which favor the nematic. Minimizing the total free energy with respect to the local ODF and q leads to following coupled set of stationarity conditions:

$$
\frac{\delta}{\delta f(\hat{\mathbf{u}})} \left(\frac{F^{\text{id}} + F^{\text{ex}}}{V} - \mu \int d\hat{\mathbf{u}} f(\hat{\mathbf{u}}) \right) = 0 \tag{10}
$$

$$
\frac{\partial}{\partial q} \left(\frac{F^{\text{id}} + F^{\text{ex}}}{V} \right) = 0, \tag{11}
$$

where μ is a Lagrange multiplier associated with the normalization constraint for the ODF ($\int d\hat{\mathbf{u}} f(\hat{\mathbf{u}}) \equiv 1$) and

$$
\frac{F^{\text{id}}}{V} = k_{\text{B}}T \int d\hat{\mathbf{u}} \rho f(\hat{\mathbf{u}})[\ln \mathcal{V}\rho f(\hat{\mathbf{u}}) - 1] \tag{12}
$$

is the exact ideal free energy of a spatially uniform system ($\mathcal{V}$ is the thermal volume of the rod). For weak twist deformations it is safe to assume that the local ODF remains unaffected by the twist and that it adopts the same form as in the nematic. Denoting $f(\hat{\mathbf{u}}) = f_0(\hat{\mathbf{u}})$, the equilibrium ODF of the nematic phase, the equilibrium value for the pitch wave vector at a given density ρ is given by the ratio of the average chiral and elastic forces[1]:

$$
q = \frac{K_t[f_0]}{K_2[f_0]}. \tag{13}
$$

The expressions for the twist parameters can be made analytically tractable by using a Gaussian trial function Ansatz to describe the local ODF[40,70]. This is done in Sec. IV. First we have to specify the form of the interaction potential and kernel Φ based on a suitable pair potential for chiral spherocylinders.

III. GENERALIZED VAN DER WAALS THEORY FOR SW RODS

Whilst the seminal view of Onsager[37] that the repulsive inflexible core of a particle gives rise to orientationally ordered phases is now very well established, the specific nature of the dispersive and polar interactions can have an important influence on the macroscopic structures that are observed. For example, in the case of hard

rods with central point dipoles, layered liquid crystalline phases such as the smectic-A are favored, while the effect on the isotropic-nematic transition appears to be small and in some cases unfavorable[71,72,73]; for molecules with terminal dipoles, the nematic phase is stabilized relative the smectic phase[74]. As can be inferred from the discussion in the introductory section, the influence of attractive interactions is all the more beguiling and subtle in the case of systems with chiral interactions, where the pitch of the helix is found to be very sensitive to the balance of forces that the molecules experience.

Let us consider an ensemble of hard spherocylinders (HSC), cylinders of length L capped by hemispheres of diameter D. The rods can be rendered chiral by introducing the simple pseudo-scalar potential, proposed by Goossens[29]. For any non-overlapping configuration of a pair of rods the chiral contribution reads

$$\Phi_{\text{chiral}} = -\varepsilon_{212} u(r_{12}) T_{212}(\hat{\mathbf{r}}_{12}; \hat{\mathbf{u}}_1, \hat{\mathbf{u}}_2), \qquad (14)$$

which consists of a radial part $u(r_{12})$ and an orientation-dependent pseudo-scalar defined as

$$T_{212}(\hat{\mathbf{r}}_{12}; \hat{\mathbf{u}}_1, \hat{\mathbf{u}}_2) = (\hat{\mathbf{u}}_1 \cdot \hat{\mathbf{u}}_2)(\hat{\mathbf{u}}_1 \times \hat{\mathbf{u}}_2 \cdot \hat{\mathbf{r}}_{12}), \qquad (15)$$

which in fact represents the first non-trivial term in a series expansion in terms of generalized chiral pseudo-scalars $T_{2i(2k-1)2j}$. For the present case of weak chiral interactions it suffices to retain only the first term. As T_{212} changes sign upon interchanging particle positions, $\hat{\mathbf{r}}_{12} \rightarrow -\hat{\mathbf{r}}_{12}$, while keeping the orientations fixed, the pseudo-scalar imparts a chiral interaction. The sign of the amplitude ε_{212} defines the handedness of the chiral interaction and the corresponding helical mesostructure.

In Goossens' model[29] the radial part decays steeply via $u(r_{12}) = 1/r_{12}^7$, which arises from a summation over electrostatic dipolar interaction sites located on each rod. Here, we employ a much simpler dependence based on a simple SW form with range λ. We thus specify $u(r_{12}) = H(\lambda - r_{12})$, with H a Heaviside step function. To take into account the effect of achiral attractive (or soft-repulsive) forces we introduce an additional achiral SW potential with amplitude (well depth) ε_{000}. For simplicity, we assume both the chiral and achiral SW potentials to have the same interaction range λ:

$$\begin{aligned} \Phi_{\text{achiral}} &= -\varepsilon_{000} H(\lambda - r_{12}) \\ \Phi_{\text{chiral}} &= -\varepsilon_{212} T_{212}(\hat{\mathbf{r}}_{12}; \hat{\mathbf{u}}_1, \hat{\mathbf{u}}_2) H(\lambda - r_{12}), \end{aligned} \qquad (16)$$

for any non-overlapping rod pair configuration. Putting all contributions together, we arrive at the following total pair potential for chiral SW rods:

$$\Phi_{\text{tot}}(\mathbf{r}_{12}; \hat{\mathbf{u}}_1, \hat{\mathbf{u}}_2) = \begin{cases} \infty & r_{12} < \sigma \\ -\varepsilon_{000} - \varepsilon_{212} T_{212} & \sigma \leq r_{12} < \lambda \\ 0 & r_{12} \geq \lambda, \end{cases} \qquad (17)$$

with $\sigma(\hat{\mathbf{r}}_{12}; \hat{\mathbf{u}}_1, \hat{\mathbf{u}}_2)$ the centre-of-mass contact distance between two hard spherocylinders at given (relative) orientations. Henceforth, we shall fix the SW range at

$\lambda = L + D$ (the so-called "square peg in a round hole" model). It is advantageous to introduce a *reduced temperature* defined as $T^* = k_B T / |\varepsilon_{000}|$. An expression for the free energy of the nematic phase of particles consisting of a hard anisotropic core with attractive interactions can be obtained from a first-order perturbation theory around a suitable hard-core reference free energy. A generalized van der Waals (GvdW) form can be expressed as[75,76,77]

$$\begin{aligned} \frac{F_{\text{GvdW}}^{\text{ex}}}{V} &= \frac{\rho^2}{2} k_B T G(\phi) \iint d\hat{\mathbf{u}}_1 d\hat{\mathbf{u}}_2 f(\hat{\mathbf{u}}_1) f(\hat{\mathbf{u}}_2) \\ &\quad \times \int d\hat{\mathbf{r}}_{12} \int_0^\sigma dr_{12} r_{12}^2 \\ &\quad - \frac{\rho^2}{2} \iint d\hat{\mathbf{u}}_1 d\hat{\mathbf{u}}_2 f(\hat{\mathbf{u}}_1) f(\hat{\mathbf{u}}_2) \\ &\quad \times \int d\hat{\mathbf{r}}_{12} \int_\sigma^\lambda dr_{12} r_{12}^2 (\varepsilon_{000} + \varepsilon_{212} T_{212}). \end{aligned} \qquad (18)$$

The first contribution is the Onsager-Parsons excess free energy accounting for the hard-core repulsive part of the pair potential. It is based upon a scaled second virial approximation according to the Parsons-Lee approach[78,79,80]. It involves a mapping of the radial distribution function for the anisotropic particles onto that of an equivalent hard-sphere system via the virial equation. The rod free energy can ultimately be linked to the Carnahan-Starling[81,82] expression for hard spheres which provides a simple strategy to account for the effect of higher-body interactions, albeit in an implicit and approximate manner. The scaling factor

$$G(\phi) = \frac{1 - \frac{3}{4}\phi}{(1 - \phi)^2}, \qquad (19)$$

reduces to unity in the Onsager limit $L/D \rightarrow \infty$ where the packing fraction ϕ of the nematic phase at the ordering transition vanishes. The second term of Eq. (18) is the contribution to the free energy due to the attractive interactions, at the mean-field level of description (i.e., any correlations in the particle positions are neglected). This type of augmented van der Waals equation of state is commonly employed in studies of homogeneous fluids (e.g., see references[83,84]), and can even be used to describe complex fluid phase equilibria in a quantitative manner (for instance the liquid-liquid phase behavior of hydrocarbons and perfluoroalkanes[85], or aqueous mixtures of hydrocarbons[86] and amphiphiles[87]).

If the GvdW excess free energy is mapped onto the general form given by Eq. (1) we can obtain the following expression for the total interaction kernel Φ:

$$\Phi(\mathbf{r}_{12}; \hat{\mathbf{u}}_1, \hat{\mathbf{u}}_2) = \begin{cases} k_B T G(\phi) & r_{12} < \sigma \\ -\varepsilon_{000} - \varepsilon_{212} T_{212} & \sigma \leq r_{12} < \lambda. \end{cases} \qquad (20)$$

It is important to note that Φ is not invariant with respect to $\mathbf{r}_{12} \rightarrow -\mathbf{r}_{12}$ as would be the case for achiral
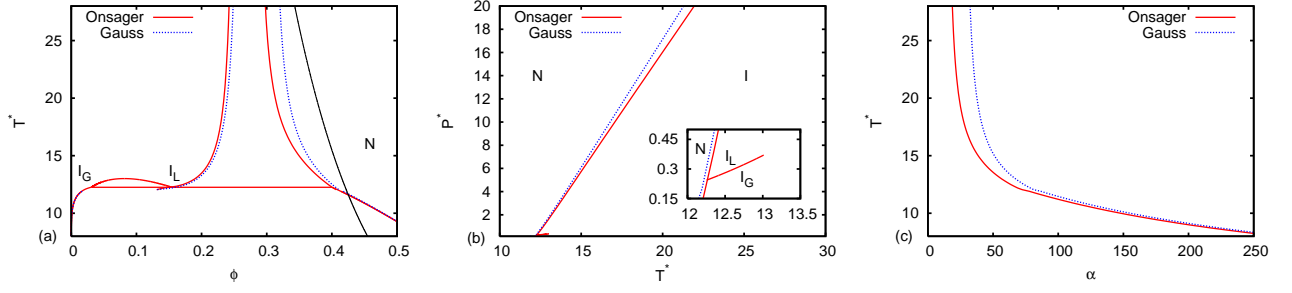
FIG. 1: Phase diagram of achiral ($\varepsilon_{212} = 0$), attractive SW spherocylinders ($\varepsilon_{000} > 0$) of aspect ratio $L/D = 10$ and range $\lambda = L+D$. The phase behavior is represented in (a) the reduced temperature $T^* = k_B T/|\varepsilon_{000}|$ versus molecular packing fraction $\phi = v_0\rho$ plane with $v_0 = (\pi/4)LD^2 + (\pi/6)D^3$ the spherocylinder volume, and (b) the reduced pressure $P^* = Pv_0/|\varepsilon_{000}|$ versus T^* plane; the continuous curve in (a) represents an isobar for $P^* = 120$. The calculations are based on the Onsager and Gaussian trial functions, Eq. (24) and Eq. (25), respectively. (c) Variational parameter α of the coexisting nematic phase versus T^*.

interactions. In the case of ranges of the SW interaction that are at least as long as the longest dimension of the particles ($L + D$) the integration of the interaction decouples neatly into a repulsive and attractive contributions; the integration is not as straightforward for shorter ranged interactions.

The fluid phase behavior for achiral attractive rods ($\varepsilon_{212} = 0$) has been discussed extensively in Refs. 76,77 and a typical example is reproduced in Fig. 1. For this calculation we only need the zeroth moment M_0 which readily follows from Eq. (9) and Eq. (20):

$$M_0(\hat{\mathbf{u}}_1, \hat{\mathbf{u}}_2) = (k_B TG(\phi)+\varepsilon_{000})v_{\text{excl}}(\gamma)-\varepsilon_{000}\frac{4\pi}{3}\lambda^3, \quad (21)$$

where v_{excl} is the excluded volume between two hard spherocylinders at a relative angle $\gamma = \arcsin|\hat{\mathbf{u}}_1 \times \hat{\mathbf{u}}_2|$:

$$\begin{aligned}
v_{\text{excl}}(\gamma) &= \frac{1}{3}\int d\hat{\mathbf{r}}_{12}\sigma^3 \\
&= 2L^2D|\sin\gamma| + 2\pi D^2L + \frac{4\pi}{3}D^3. \quad (22)
\end{aligned}$$

The ODF $f_N(\hat{\mathbf{u}})$ of the nematic state is formally given by the solution of the self-consistency equation emerging from Eq. (10):

$$f_N(\hat{\mathbf{u}}) = \frac{\exp\left[-\rho\int d\hat{\mathbf{u}}' M_0(\hat{\mathbf{u}}, \hat{\mathbf{u}}')f_N(\hat{\mathbf{u}}')\right]}{\int d\hat{\mathbf{u}}\exp\left[-\rho\int d\hat{\mathbf{u}}' M_0(\hat{\mathbf{u}}, \hat{\mathbf{u}}')f_N(\hat{\mathbf{u}}')\right]}, \quad (23)$$

which is not amenable to further analysis and is solved numerically. The double orientational averages appearing in Eq. (18) can be made analytically tractable by adopting a simple algebraic trial form for the ODF. In his original paper Onsager[37] introduced the following form to describe the distribution of angles in the uniaxial nematic state:

$$f_O(\theta) = \frac{\alpha\cosh(\alpha\cos\theta)}{4\pi\sinh\alpha}, \quad (24)$$

where $\cos\theta = \hat{\mathbf{u}} \cdot \hat{\mathbf{n}}$ is the polar angle between the axis of symmetry of the particle and the director and $\alpha \geq 0$

a variational parameter measuring the degree of nematic order. Note that $\alpha \equiv 0$ in the isotropic phase. The implications of Eq. (24) on the GvdW free energy have been studied in detail in Ref. 77. A simpler trial function has been proposed by Odijk and Lekkerkerker[70], based on a Gaussian:

$$f_G(\theta) = \frac{\alpha}{4\pi}\exp\left(-\frac{1}{2}\alpha\theta^2\right) \qquad 0 \leq \theta \leq \pi/2, \quad (25)$$

and its mirrored version for the interval $\pi/2 \leq \theta \leq \pi$. Unlike Eq. (24), the Gaussian trial form does not reduce to the correct isotropic constant $1/4\pi$ for $\alpha = 0$ and we must therefore require $\alpha \gg 1$ for reasons of consistency. In fact, Eq. (24) becomes identical to the Gaussian form in the asymptotic limit $\alpha \to \infty$. The results from both distributions will therefore be virtually indistinguishable for large α, as is illustrated in Fig. 1c.

Let us quote the following Gaussian averages[70]:

$$\begin{aligned}
\langle \ln f(\hat{\mathbf{u}})\rangle &\sim \ln 4\pi\alpha - 1 \\
\langle\langle\sin\gamma\rangle\rangle &\sim \left(\frac{\pi}{\alpha}\right)^{1/2} \quad (\alpha \gg 1), \quad (26)
\end{aligned}$$

where the brackets denote orientational averages:

$$\begin{aligned}
\langle\cdot\rangle &= \int d\hat{\mathbf{u}}f_G(\hat{\mathbf{u}}), \\
\langle\langle\cdot\rangle\rangle &= \iint d\hat{\mathbf{u}}_1 d\hat{\mathbf{u}}_2 f_G(\hat{\mathbf{u}}_1)f_G(\hat{\mathbf{u}}_2). \quad (27)
\end{aligned}$$

The nematic order parameter S can be approximated by:

$$S \equiv \langle\mathcal{P}_2(\cos\theta)\rangle \sim 1 - \frac{3}{\alpha}, \quad (28)$$

with $\mathcal{P}_2$ the second-order Legendre polynomial. Using the asymptotic expressions from Eq. (26) in the ideal and excess free energy yields a simple algebraic expression for the free energy. The corresponding phase equilibria can be analyzed without difficulty and the resulting

phase diagrams are shown in Fig. 1; the coexisting densities are obtained by numerically solving the equality of pressure $P_i = -(\partial F/\partial V)_{N,T}$ and chemical potential $\mu_i = -(\partial F/\partial N)_{V,T}$ of each phase i. At low to moderate temperatures, a coexistence between isotropic gas (I_G) and liquid (I_L) phases is found in addition to the isotropic-nematic phase separation seen at higher densities. At the triple point temperature $T^* = 12.254$ the isotropic liquid binodal meets a triphasic I_G-I_L-N equilibrium line. For systems with chiral interactions ($\varepsilon_{212} \neq 0$) the phase behavior is altered by the twist contributions which we shall examine in the next Section.

IV. CALCULATION OF THE TWIST PARAMETERS

The central task in the description of chiral nematic phases within our GvdW theory is the calculation of the moment integrals pertaining to the twist energy and elastic modulus in Eq. (7) and Eq. (8) using the explicit interaction kernel defined in Eq. (20). Details of the specific treatment are provided in the next subsections.

A. Twist elastic modulus

The calculation of the twist elastic modulus consists of two steps. First, an explicit expression for the second moment M_2 in Eq. (9) is required. Then, a double orientational average has to be carried out using an appropriate form for the ODF according to Eq. (8). Inserting Eq. (20) into Eq. (9) and rearranging terms leads to

$$M_2(\hat{\mathbf{u}}_1, \hat{\mathbf{u}}_2) = (k_B T G(\phi) + \varepsilon_{000}) \int_{v_{\text{excl}}} d\mathbf{r}_{12} z_{12}^2$$
$$-\varepsilon_{000} \int_\lambda d\mathbf{r}_{12} z_{12}^2 + \mathcal{O}(\varepsilon_{212}), \quad (29)$$

where $\int_{v_{\text{excl}}} d\mathbf{r}_{12} = \int d\hat{\mathbf{r}}_{12} \int_0^\sigma dr_{12} r_{12}^2$ denotes a spatial integral over the spherocylinder excluded volume and $\int_\lambda d\mathbf{r}_{12} = \int d\hat{\mathbf{r}}_{12} \int_0^\lambda dr_{12} r_{12}^2$ a spatial integration over the SW range. All contributions of $\mathcal{O}(\varepsilon_{212})$ are of negligible importance for weak chirality; more specifically, the ratio of the chiral and non-chiral interactions must be small, i.e.,

$$\epsilon_c = \left| \frac{\varepsilon_{212}}{\varepsilon_{000}} \right| \ll 1, \quad (30)$$

where one should also note that $G(\phi) > 1$. The *chirality parameter* ϵ_c is, in principle, fixed by the detailed molecular structure of the rod-like mesogen and is expected to be small for most common chiral substances. In the case of strong chiral interactions, $[\epsilon_c \sim \mathcal{O}(1)]$, the twist elastic response will be affected by T_{212} (and higher order pseudo-scalar potentials) which severely complicates the analysis. The second integral in Eq. (29) is easily evaluated by exploiting the symmetry of the SW potential along the z-axis and using cylindrical coordinates:

$$\int_\lambda d\mathbf{r}_{12} z_{12}^2 = 2\pi \int_{-\lambda}^\lambda dz_{12} z_{12}^2 \int_0^{\sqrt{\lambda^2 - z_{12}^2}} dr\, r = \frac{4\pi\lambda^5}{15}, \quad (31)$$

where $r = (x_{12}^2 + y_{12}^2)^{1/2}$. The first term in Eq. (29) involves a weighted spatial integral over the excluded-volume manifold spanned by two spherocylinders at fixed orientations. Details of this calculation can be found in Appendix A. The final expression for M_2 reads:

$$M_2(\hat{\mathbf{u}}_1, \hat{\mathbf{u}}_2) = (k_B T G(\phi) + \varepsilon_{000}) \left[L^2 D |\sin\gamma| \frac{2}{3} \left(A_1^2 + A_2^2 + B^2 \right) \right.$$
$$\left. + L D^2 \left\{ \frac{16}{3}(A_1 C_2 - A_2 C_1) + \frac{8\pi}{3}(A_1^2 + A_2^2) + \pi B^2 + \frac{\pi}{2}(C_1^2 + C_2^2) \right\} + v_{M_2}^{HH} \right] - \frac{4\pi\varepsilon_{000}\lambda^5}{15}, \quad (32)$$

where $v_{M_2}^{HH} \propto \mathcal{O}(D^5)$ is given by Eq. (68) in Appendix A. The second moment excluded volume is independent of the chiral interaction in the limit of infinitesimally small twist distortions considered here. In Eq. (32), A_i, B and C_i are orientationally dependent dot products specified in Eq. (65) of Appendix A.

The elastic modulus is obtained from a double orientational average of M_2 for which we shall invoke a Gaussian trial function for the ODF, *cf.* Eq. (25). In principle a twist deformation of the director field breaks the uniaxial symmetry of the local ODF, which would now take on a biaxial form, and a suitable generalization of the Gaussian distribution involving an explicit dependence on the azimuthal angle would therefore be required. To keep the theory tractable, we shall ignore local biaxiality and use the original form of Eq. (25). As the degree of biaxial

nematic order is very small in the weak deformation limit considered here, it is unlikely to have a significant effect on the mesoscopic properties of the cholesteric phase.

Since the Gaussian ODF is only appropriate if the orientational distribution is strongly peaked around the nematic director we may perform an asymptotic expansion of the Gaussian integrals to extract the leading order contributions for large α. Let us fix $\hat{\mathbf{z}} = \{0, 0, 1\}$ and introduce

$$\hat{\mathbf{u}}_i = \{\cos \theta_i, \sin \theta_i \cos \varphi_i, \sin \theta_i \sin \varphi_i\}, \qquad (33)$$

the orientational unit vector of rod $i = 1, 2$ in terms of the polar (θ_i) and azimuthal (φ_i) angle with respect to the nematic director which we have fixed along the x-direction of the Cartesian frame $\hat{\mathbf{n}} = \hat{\mathbf{x}} = \{1, 0, 0\}$. Expanding the dot products in Eq. (65) for $\theta_i \ll 1$ we obtain up to leading order:

$$|\sin \gamma| \sim |\gamma| \sim \left(\theta_1^2 + \theta_2^2 - 2\theta_1 \theta_2 \cos \Delta \varphi \right)^{1/2} \quad (34)$$
$$A_i \sim (L/2) \theta_i \sin \varphi_i$$
$$B \sim D(\theta_2 \cos \varphi_2 - \theta_1 \cos \varphi_1)/|\gamma|$$
$$C_1 = C_2 \sim D(\theta_1 \sin \varphi_1 - \theta_2 \sin \varphi_2)/|\gamma|, \qquad (35)$$

with $\Delta \varphi = \varphi_2 - \varphi_1$. The twist elastic modulus can be recast into a finite series in terms of the inverse aspect ratio $x = D/L$:

$$\frac{K_2 D}{k_{\mathrm{B}} T} \sim -c^2 \xi \left\{ H_0 + H_1 x + H_2 x^2 + H_3 x^3 + H_4 x^4 \right\}$$
$$+ c^2 \varepsilon_{000} \lambda^5 H_\varepsilon, \qquad (36)$$

with $c = \rho L^2 D$ the dimensionless rod concentration and

$$\xi = G(\phi) \pm \frac{1}{T^*}, \qquad (37)$$

where $(+)$ applies to an attractive square-well ($\varepsilon_{000} > 0$) and $(-)$ a soft-repulsive square-shoulder ($\varepsilon_{000} < 0$) potential. The coefficients H_k represent double Gaussian averages involving the following angular quantities up to leading order in $\alpha \gg 1$:

$$H_0 \sim \frac{\alpha^2}{12} \left\langle\left\langle \mathcal{G} |\gamma| (\theta_1^2 \sin^2 \varphi_1 + \theta_2^2 \sin^2 \varphi_2) \right\rangle\right\rangle + \cdots$$

$$H_1 \sim \frac{\pi \alpha^2}{3} \left\langle\left\langle \mathcal{G} (\theta_1^2 \sin^2 \varphi_1 + \theta_2^2 \sin^2 \varphi_2) \right\rangle\right\rangle + \cdots$$

$$H_2 \sim \frac{\alpha^2}{3} \left\langle\left\langle \mathcal{G} (\theta_2 \cos \varphi_2 - \theta_1 \cos \varphi_1)^2 / |\gamma| \right\rangle\right\rangle$$
$$+ \frac{4\alpha^2}{3} \left\langle\left\langle \mathcal{G} (\theta_1 \sin \varphi_1 - \theta_2 \sin \varphi_2)^2 / |\gamma| \right\rangle\right\rangle + \cdots$$

$$H_3 \sim \frac{\pi \alpha^2}{2} \left\langle\left\langle \mathcal{G} (\theta_2 \cos \varphi_2 - \theta_1 \cos \varphi_1)^2 / \gamma^2 \right\rangle\right\rangle$$
$$+ \frac{\pi \alpha^2}{2} \left\langle\left\langle \mathcal{G} (\theta_1 \sin \varphi_1 - \theta_2 \sin \varphi_2)^2 / \gamma^2 \right\rangle\right\rangle + \cdots$$

$$H_4 \sim \frac{2\pi \alpha^2}{15} \left\langle\left\langle \mathcal{G} \right\rangle\right\rangle + \cdots$$

$$H_\varepsilon \sim \frac{2\pi \alpha^2}{15} \left\langle\left\langle \mathcal{G} \right\rangle\right\rangle = 0, \qquad (38)$$

where

$$\mathcal{G} \sim \theta_1 \theta_2 \cos \varphi_1 \cos \varphi_2 + \cdots \qquad (39)$$

The brackets represent the following four-fold angular integral:

$$\left\langle\left\langle \cdot \right\rangle\right\rangle \sim \alpha^2 \prod_{i=1,2} \int_0^\infty d\theta_i \theta_i \exp \left[-\frac{\alpha}{2} \theta_i^2 \right] \int_0^{2\pi} \left(\frac{d\varphi_i}{2\pi} \right), \qquad (40)$$

where we have used $\dot{f}_G = \partial f_G / \partial(\cos \theta) \sim \alpha f_G$. It is evident that H_ε vanishes upon integration over the azimuthal angles, irrespective of the form of the (uniaxial) ODF. A little inspection shows that the leading order contributions to H_1 and H_4 are also eliminated by the double azimuthal integration. The remaining terms are, in principle, nonzero because $|\gamma|$ depends non-randomly on $\Delta \varphi$. The results can be greatly simplified by changing to the new azimuthal variables $\varphi_1 = \psi$ and $\varphi_2 = \psi + \Delta \varphi$. The integration over ψ can be carried out without difficulty. After some algebra the averages reduce to:

$$H_0 \sim \frac{\alpha^2}{96} \left\langle\left\langle \theta_1 \theta_2 (\theta_1^2 + \theta_2^2) |\gamma| \cos \Delta \varphi \right\rangle\right\rangle + \cdots$$

$$H_2 \sim \frac{\alpha^2}{24} \left\langle\left\langle \theta_1 \theta_2 \left[(\theta_1^2 + \theta_2^2) 7 \cos \Delta \varphi \right. \right.\right.$$
$$\left.\left.\left. - (4 + 10 \cos 2\Delta \varphi) \right] / |\gamma| \right\rangle\right\rangle + \cdots$$

$$H_3 \sim \frac{\pi \alpha^2}{4} \left\langle\left\langle \theta_1 \theta_2 \cos \Delta \varphi \right\rangle\right\rangle + \cdots \qquad (41)$$

Here, the brackets now denote Eq. (40) with the double azimuthal integral over $\varphi_{1,2}$ replaced by a single one over the remaining angle $\Delta \varphi$. Clearly, the azimuthal average yields $H_3 = 0$ so that we need only evaluate the two even contributions H_0 and H_2. The first term corresponding to infinitely long rods has been analyzed by Odijk in Ref. 88. Eliminating $\cos \Delta \varphi$ via the asymptotic expression for $|\sin \gamma|$ [Eq. (34)] leads to:

$$H_0 \sim \frac{\alpha^2}{96} \left[-\left\langle\left\langle |\gamma|^3 \theta_1^2 \right\rangle\right\rangle + \left\langle\left\langle |\gamma| \theta_1^2 (\theta_1^2 + \theta_2^2) \right\rangle\right\rangle \right] \qquad (42)$$

We may now use the Gaussian averages in Appendix B to arrive at the compact expression,

$$H_0 \sim -\frac{7}{192} \left(\frac{\pi}{\alpha} \right)^{1/2} \qquad (43)$$

Similarly, by applying Eq. (34) to H_2 we may simplify:

$$H_2 \sim \frac{\alpha^2}{24} \left[\frac{13}{24} \left\langle\left\langle |\gamma| \theta_1^2 \right\rangle\right\rangle - \frac{5}{24} \left\langle\left\langle |\gamma|^3 \right\rangle\right\rangle \right.$$
$$\left. + \frac{1}{8} \left\langle\left\langle \theta_1^2 (\theta_2^2 - \theta_1^2) / |\gamma| \right\rangle\right\rangle \right]. \qquad (44)$$

The first two Gaussian averages are given in Appendix B. The last one cannot be calculated analytically, but the α dependence is easily established from a simple analysis of

the scaling, while the pre-factor can be found numerically (see Appendix B). The final result is:

$$H_2 \sim -\kappa \alpha^{1/2}, \qquad (45)$$

with $\kappa = 0.036926$. For later reference, we also give the next leading order α-contributions to H_k. It can be shown that the odd terms H_1 and H_3 in Eq. (38) are fully eliminated (to all order in α) by the double azimuthal integration. The higher order α-contributions to H_k (even k) are in principle non-vanishing and can be estimated by considering the angular quantities in Eq. (38) taking the next power in the polar angle θ_i. From simple scaling considerations it then follows that the corrections δH_k must be at least of order:

$$\begin{aligned}
\delta H_0 &\sim \mathcal{O}(\alpha^{-1}), \\
\delta H_2 &\sim \mathcal{O}(\alpha^{-1/2}), \\
\delta H_4 &\sim \mathcal{O}(\alpha^{1/2}).
\end{aligned} \qquad (46)$$

which all give marginal contributions to K_2 for large aspect ratio.

The equilibrium value for α is obtained from the reference free energy of the (undistorted) nematic. Combining the ideal and excess parts of the nematic free energy, Eq. (12) and Eq. (6) respectively, with the expression for M_0 [Eq. (21)] gives:

$$\frac{F^{\mathrm{GvdW}}}{k_{\mathrm{B}}TN} = \langle \ln \mathcal{V}\rho f(\hat{\mathbf{u}}) - 1 \rangle + \frac{\rho \xi}{2} \langle\langle v_{\mathrm{excl}}(\hat{\mathbf{u}}_1, \hat{\mathbf{u}}_2) \rangle\rangle + \frac{2\pi \rho \lambda^3}{3T^*}. \qquad (47)$$

On inserting the Gaussian averages for the ideal and excluded volume contributions [Eq. (26)], the asymptotic free energy becomes

$$\frac{F^{\mathrm{GvdW}}}{k_{\mathrm{B}}TN} \sim \ln \alpha + c\xi(\pi/\alpha)^{1/2}, \qquad (48)$$

where all terms independent of α have been omitted for compactness as they do not contribute to the degree of orientational order. Minimizing the free energy with respect to α yields the common quadratic form[89]:

$$\alpha \sim (\pi^{1/2}c\xi/2)^2. \qquad (49)$$

With this relation for α, an *algebraic* expression for the twist elastic constant for the SW spherocylinders can be formulated from Eq. (36). After defining the spherocylinder packing fraction as $\phi \simeq (\pi/4)xc$ (ignoring the end-cap corrections), we obtain

$$K_2^* = \frac{K_2 D}{k_{\mathrm{B}}T}x \sim \phi \left\{ \frac{7}{24\pi} + \frac{32}{\pi^{5/2}}\kappa(\phi\xi)^2 + \mathcal{O}(x) \right\}. \qquad (50)$$

The twist elastic modulus primarily depends on the particle packing fraction and the reduced temperature, with the aspect ratio merely playing the role of a linear scaling factor.

Some remarks are now in order. The leading order contribution was found for infinitely thin rods[88] and does
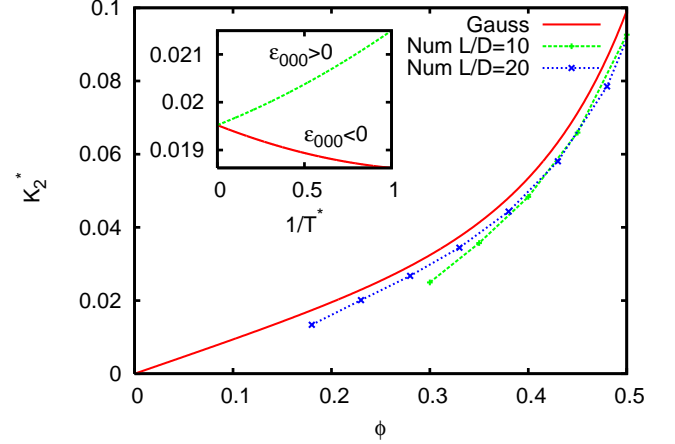

FIG. 2: Twist elastic modulus $K_2^* = K_2 Dx/k_{\mathrm{B}}T$ [Eq. (50)] for hard spherocylinders ($1/T^* = 0$) as a function of packing fraction $\phi = v_0\rho$. The numerical ODF is given by the solution of Eq. (23). Inset: Temperature dependence of K_2^* for rods of aspect ratio $L/D = 20$ with attractive square-well ($\varepsilon_{000} > 0$) and soft-repulsive square-shoulder ($\varepsilon_{000} < 0$) interactions of range $\lambda = L + D$ at a fixed packing fraction of $\phi = 0.2$.

not depend on temperature. The twist elastic modulus is *independent* of the range λ of the SW potential. Correction terms arising from the next leading order terms in Eq. (46) are at least of order $x = D/L$ and thus of marginal influence for sufficiently slender rods. Fig. 2 shows that the discrepancy with numerical results is very small even for relatively short rods with $L/D = 10$. The numerical data are based on a numerical evaluation of Eq. (8) using the exact ODF from Eq. (23). It is important to note that the cholesteric phase is only stable with respect to the isotropic state roughly when $c \gtrsim 1$ or equivalently $\phi \gtrsim x$. As illustrated in Fig. 2, numerical results for the nematic solution of the ODF Eq. (23) are found only above a critical packing fraction.

As expected, the twist elastic modulus is a monotonically increasing function of the packing fraction. The temperature dependence shown in Fig. 2 indicates an increase of the twist elastic resistance for attractive rods ($\varepsilon_{000} > 0$), while the opposite trend is observed for a soft-repulsive square-shoulder potential ($\varepsilon_{000} < 0$). The latter interaction may be particularly suitable for the description of colloidal fd-virus rods as a crude model for the electric double layer or the polymer coat grafted onto the colloid surface[16].

The behavior of the twist elastic modulus with respect to the nematic order parameter is highlighted in Fig. 3. Since $\alpha \sim \phi^2$ [Eq. (49)] and $\alpha \sim 1/(1-S)$ [Eq. (28)] it is readily deduced that the asymptotic behavior of the twist elastic modulus for strong nematic order is given by the following scaling relation:

$$K_2^* \sim a \left(\frac{1}{1-S} \right)^{1/2} + b \left(\frac{1}{1-S} \right)^{3/2}, \qquad (51)$$
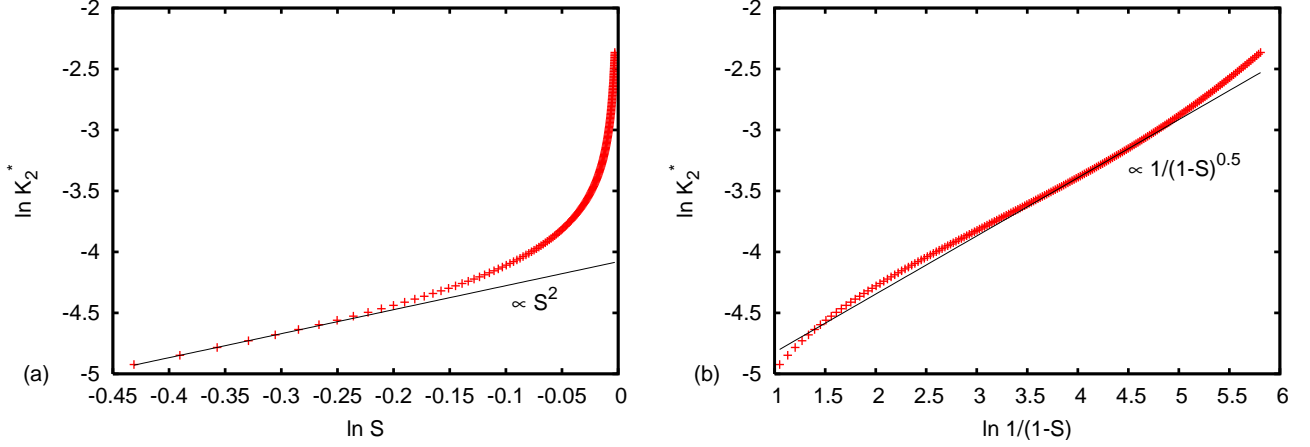
FIG. 3: Scaling of the twist elastic modulus K_2^* with respect to the nematic order parameter S. The results are obtained from the numerical ODF [Eq. (23)] using $L/D = 20$. Continuous lines represent linear fits. (a) Quadratic behavior $K_2^* \sim S^2$ at moderate nematic order $0.6 < S < 0.9$. (b) Asymptotic behavior $K_2^* \sim 1/(1-S)^\omega$ with $\omega \geq 0.5$ in the regime of high nematic order ($S > 0.99$).

in terms of the constants a and b. This scaling relation is confirmed in Fig. 3b based on numerical results for the twist elastic modulus[48]. The crossover between the two scaling contributions in Eq. (51) is reflected by the fact that the exponent $[1/(1-S)^\omega]$ lies within the range $0.5 < \omega < 1.5$ as S approaches unity (or equivalently $1/(1-S) \to \infty$). A different scaling behavior is observed for moderate nematic order where K_2^* is found to be proportional to S^2 (Fig. 3a). This result is in agreement with previous theoretical predictions based on a Legendre series expansion of the angular properties valid for weak nematic order[45,50].

B. Twist energy

We proceed in a similar manner for the calculation of the twist energy. The first-moment spatial integral over the interaction kernel Eq. (20) is required first. None of the terms pertaining to the achiral parts of the interaction potential contribute to the twist energy so that

$$M_1(\hat{\mathbf{u}}_1, \hat{\mathbf{u}}_2) = \varepsilon_{212} \int_{v_{\text{excl}}} d\mathbf{r}_{12} z_{12} T_{212}$$
$$-\varepsilon_{212} \int_\lambda d\mathbf{r}_{12} z_{12} T_{212}, \qquad (52)$$

The second spatial integral is easily tackled by switching to cylindrical coordinates. Let us write $\mathbf{r}_{12} = r \sin\beta \hat{\mathbf{x}} +$

$r \cos\beta \hat{\mathbf{y}} + z_{12} \hat{\mathbf{z}}$ so that

$$\int_\lambda d\mathbf{r}_{12} z_{12} T_{212} = \int_0^{2\pi} d\beta \int_{-\lambda}^\lambda dz_{12} z_{12}$$
$$\times \int_0^{\sqrt{\lambda^2 - z_{12}^2}} dr r T_{212}$$
$$= \frac{\pi}{3} \lambda^4 (\hat{\mathbf{u}}_1 \cdot \hat{\mathbf{u}}_2)(\hat{\mathbf{u}}_1 \times \hat{\mathbf{u}}_2 \cdot \hat{\mathbf{z}}). \quad (53)$$

The first spatial integral runs over the excluded volume of the spherocylinder for which we use the parametrization advanced in Appendix A. This produces terms of $\mathcal{O}(LD^3)$ and higher order in D which we will not show explicitly. We can thus write the first-moment integral as the following expression:

$$M_1(\hat{\mathbf{u}}_1, \hat{\mathbf{u}}_2) = -\frac{\pi}{3}\varepsilon_{212}\lambda^4(\hat{\mathbf{u}}_1 \cdot \hat{\mathbf{u}}_2)(\hat{\mathbf{u}}_1 \times \hat{\mathbf{u}}_2 \cdot \hat{\mathbf{z}}) + \mathcal{O}(LD^3).$$
$$(54)$$

Inserting the asymptotic forms of $\hat{\mathbf{u}}_i$ for small polar angles into Eq. (7) and performing the azimuthal integration over φ_1 one can express the chiral torque as

$$\frac{K_t D^2}{k_B T} \sim \frac{\pi}{6} c^2 \varepsilon_{212} \left(\frac{\lambda}{L}\right)^4 \alpha \left\langle -\theta_2^2 \cos^2 \varphi_2 \right\rangle + \mathcal{O}(x^3)$$
$$\sim \frac{\pi}{6} \frac{\epsilon_c}{T^*} c^2 \left(\frac{\lambda}{L}\right)^4 + \mathcal{O}(x^3), \qquad (55)$$

where the elementary Gaussian average $\langle \theta^2 \cos^2 \varphi \rangle \sim 1/\alpha$ has been employed. This expression is similar to the one derived for infinitely thin rods[88]. The correction terms due to finite rod thickness are deemed to be very small, and can be ignored if the spherocylinders are not too short.

C. Cholesteric pitch

A microscopic expression for the cholesteric pitch of SW spherocylinders in the limit of weak twist distortion is obtained by combining Eq. (50) and Eq. (55) in Eq. (13). After some rearranging one can write the pitch $p = 2\pi/q$ in a convenient reduced form as

$$
\begin{aligned}
p^* &= \left(\frac{p}{L}\right)\bar{\epsilon} \\
&\sim \frac{T^*}{\phi}\left\{\frac{7\pi}{32} + \frac{24\kappa\phi^2}{\pi^{1/2}}\left(G(\phi) \pm \frac{1}{T^*}\right)^2 + \mathcal{O}(x)\right\}, \quad (56)
\end{aligned}
$$

where $(+)$ refers to a square-well and $(-)$ to a square-shoulder potential. The factor $\bar{\epsilon}$ scaling the pitch combines the chirality parameter ϵ_c and the geometric parameters of the range λ and (inverse) aspect ratio $x = D/L \ll 1$. It can be interpreted as an integrated van der Waals energy which depends on the fourth power of the (SW) interaction range λ:

$$
\bar{\epsilon} = \frac{\epsilon_c}{x^2}\left(\frac{\lambda}{L}\right)^4. \quad (57)
$$

As with the twist elastic modulus, Eq. (50), the rescaled pitch depends only on the packing fraction and reduced temperature of the cholesteric phase.

V. RESULTS AND DISCUSSION

The density and temperature dependence of the cholesteric pitch obtained with the theory presented in the previous sections is depicted in Fig. 4. The variation of the pitch with packing fraction is non-monotonic, irrespective of the reduced temperature. The steep decrease at low densities is a common result for slender rods. Since $K_t \propto \phi^2$ and $K_2 \propto \phi$ [cf. Eq. (55) and Eq. (50)], the free-energy cost associated with the elastic deformation upon incrementing the density is more than offset by the simultaneous free energy gain due to an increase of the torque-field associated with the chiral interactions. The inverse proportionality $p \propto \phi^{-1}$ is in agreement with Odijk's result for rigid rods[40] and consistent with experimental results of fd-rods at high ionic strength[16]. At higher packing fractions, the orientational (nematic) order rises sharply and the influence of the finite rod thickness, embodied by the second term in Eq. (56), becomes apparent. The elastic resistance rises steeply and causes the cholesteric structure to unwind upon increasing density.

For large temperatures $(1/T^* < 1)$, the behavior of the pitch is only weakly affected by the nature of the non-chiral interactions as can be inferred from the last term in Eq. (56). From a qualitative point of view, the behavior is therefore the same for attractive square-well and soft repulsive square-shoulder potentials. Moreover, since $p^* \propto T^*$, the temperature merely serves as a linear scaling factor and does not influence the shape of the curve in Fig. 4a.

It has been suggested that the increase of the pitch with density is due to pre-smectic fluctuations that counteract the twist deformation[1,59,90]. The present analysis would suggest that the observation can be accounted for within a simple mean-field theory for anisotropic yet homogeneous systems in which one disregards density fluctuations; layered structures such as the smectic-A (SmA) phase possess inhomogeneities in the average particle position. That smectic fluctuations are not necessary to give rise to an increase in the pitch is also supported by experimental observations in colloidal fd-rods[15] where an unwinding of the cholesteric is observed at densities far below the cholesteric-smectic transition density. We stress that parallel configurations (induced by the finite rod thickness, i.e., spherocylindrical shape) that lead to an unwinding of the cholesteric state with increasing density also facilitate the formation of a smectic-A phase. The two phenomena are therefore expected to be correlated. The possibility of a transition towards a smectic phase is not incorporated in our theory but it is anticipated that such an instability would lead to a much steeper increase and possibly a divergence of the pitch with density. Based on the phase diagram of pure hard spherocylinders[91,92] the cholesteric-smectic transition would occur at a packing fraction of $\phi \sim 0.4$, irrespective of the aspect ratio (for sufficiently long rods). The unwinding of the cholesteric phase at high densities is not unique to the fd system but has also observed in solutions of polysaccharide and polypeptide compounds[18] and DNA[12,14]. Theoretically, such a trend was first established in simulations based on the chiral hard spherocylinders[93], supplemented by a simple ground-state theory for a chiral hard Gaussian overlap model assuming perfect local nematic order[38].

The temperature dependence of the pitch is also highly non-monotonic. The near linear increase of the pitch with temperature for a system at constant density (or pressure) is a direct result of the achiral hard-core repulsion between the rods which dominates the (chiral) attractive interactions at moderate to high temperatures. At $T \to \infty$ the free energy of the system is governed entirely by the entropic contribution associated with hard spherocylinders, resulting in a nematic phase $(p \to \infty)$. The unwinding of the pitch with temperature has been found in solutions of polypeptides[17], and most notably for aqueous suspensions of fd-virus rods[15] which was not accompanied by a thermal change in the intrinsic chirality of the viral structure (e.g., due to a denaturation of the protein coating). Theoretically, this would translate to a chirality parameter ϵ_c which is constant, as we have assumed here. Our predictions of an increase in pitch with increasing temperature are also consistent with the findings for the cholesterol ester CEEC[60], a thermotropic mesogen which does not exhibit a smectic phase.

The marked increase in pitch at low temperatures is in accordance with experimental observations in numer-
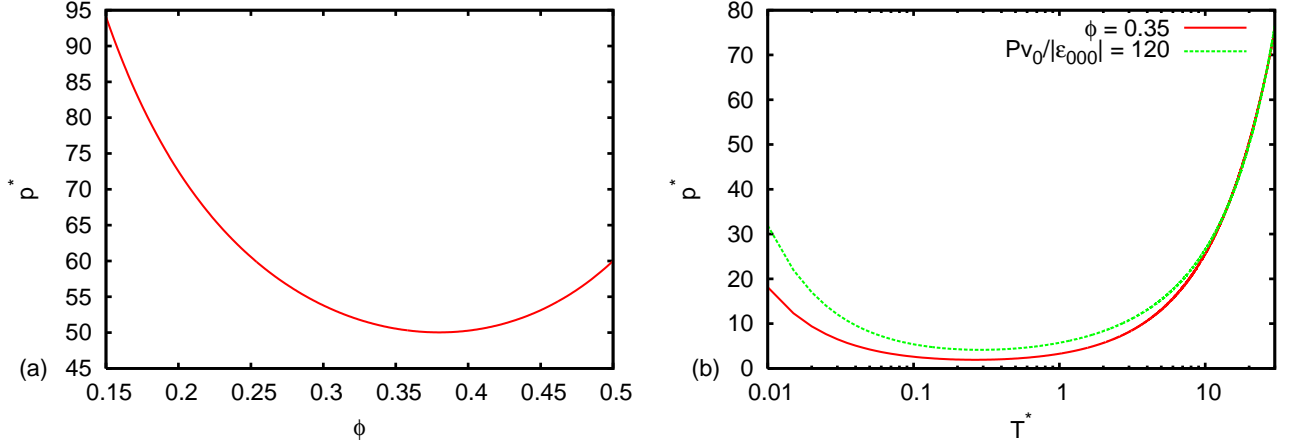
FIG. 4: (a) Scaled cholesteric pitch $p^* = (p/L)\bar{\epsilon}$ [Eq. (56)] for attractive SW spherocylinders at reduced temperature $T^* = k_BT/|\varepsilon_{000}| = 20$ versus rod packing fraction $\phi = v_0\rho$. (b) Variation of the scaled pitch as a function of T^* (on a logscale) for a constant packing fraction $\phi = 0.35$. Also shown is the behavior for a fixed rescaled pressure $P^* = Pv_0/|\varepsilon_{000}| = 120$ corresponding to the isobar (thin continuous curve) in Fig. 1a.
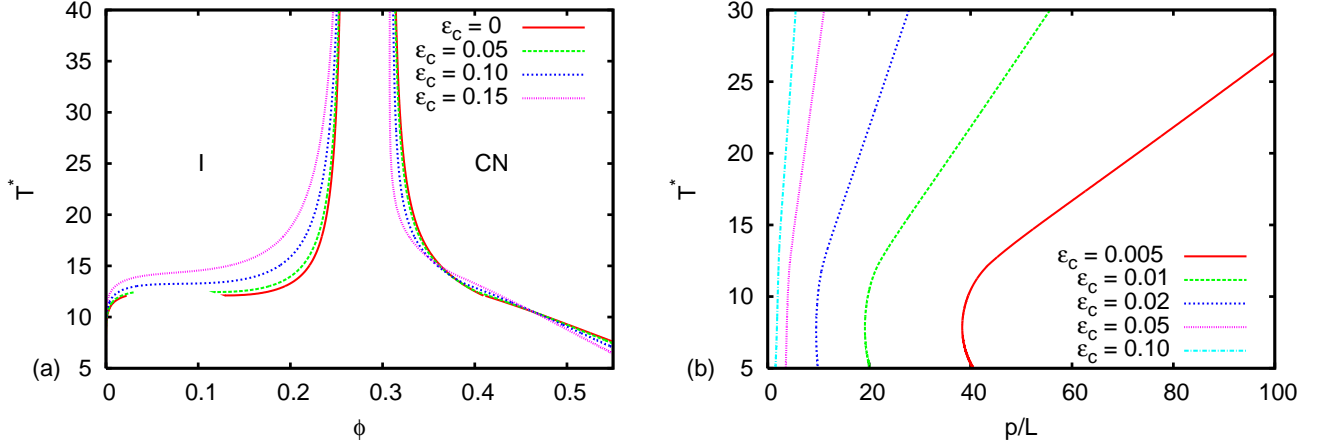

FIG. 5: (a) Phase diagram for attractive chiral SW spherocylinders ($L/D = 10$) of range $\lambda = L + D$ for various relative strengths of the chiral interaction $\epsilon_c = |\varepsilon_{202}/\varepsilon_{000}|$, where $T^* = k_BT/|\varepsilon_{000}|$ is the reduced temperature and $\phi = v_0\rho$ the packing fraction. CN denotes the cholesteric phase. (b) Temperature dependence of the reduced pitch $p^* = p/L$ of the cholesteric phase in coexistence with the isotropic.

ous thermotropic systems the most ubiquitous being the derivatives of cholesterol[59,90]. A similar trend albeit less prominent is found for aqueous solutions of fd virus[15]. The underlying scenario is analogous to the unwinding of the cholesteric with increasing density for the lyotropic case and originates from a stark increase in nematic order upon lowering T^*. The twist elastic resistance associated with the near-parallel configurations becomes anomalously large and gives rise to a strong unwinding of the cholesteric structure. As for the behavior with density, an additional coupling and a divergent pitch is expected at the nematic-smectic transition temperature as observed by Pindak et $al.$[59] and theoretically advanced by de Gennes[94]. We do point out that in our particular model the decrease of the pitch with temperature (and

constant density or pressure) observed at low temperatures is metastable with respect to an isotropic (gas)-cholesteric phase separation (see the phase diagram in Fig. 1a).

Finally, from Eq. (56) one can obtain a simple relation between the pitch and the particle aspect ratio, $p/L \propto x^2$, or equivalently $p \propto 1/L$. The pitch of the cholesteric thus becomes tighter upon increasing the aspect ratio at a fixed mass density and temperature. This result is in line with observations in fd systems where the pitch is found to decrease for larger viral contour lengths[16]. The relation found in experiment, $p \propto 1/L^{0.25}$, reveals a much weaker dependency which could be attributed to the slight degree of flexibility, neglected in the present rigid-rod model. It is noteworthy that the Straley-Odijk

theory[39,40] predicts the opposite trend $p \propto L$. Their model is based on short-ranged (steric) chiral interactions induced by a thin helical thread of thickness D enveloping the rod. Here, the chiral interactions are long-ranged and scale with the rod length $\lambda \propto L$. A linear increase in the pitch with aspect ratio is predicted with a scaled Onsager theory for chiral hard Gaussian overlap rods with the approximation of perfect local nematic order[38]. Although no microscopic justification for our scaling relation can be given, it does give the correct scaling of the pitch with contour length and is consistent with the long-ranged nature of the chiral forces between fd virus rods[16].

In Fig. 5 we shows that there is noticeable effect on the phase behavior of attractive SW spherocylinders for weakly chiral interactions. Upon increasing the strength of the chiral interaction relative to the dispersion forces (ϵ_c) the isotropic-cholesteric transition shifts to lower densities with an additional broadening of the two-phase coexistence region at moderate to high temperatures. Beyond a certain critical value, the isotropic gas-liquid envelope and the corresponding triple point become metastable relative to the direct coexistence between a low-density isotropic and a high density cholesteric phase. Since the chiral interactions are essentially attractive, we observe the same stabilization of the cholesteric state for repulsive square-shoulder potentials. The non-monotonic behavior of the pitch with temperature is reflected in Fig. 5 where the evolution of the pitch of the coexisting cholesteric phase is depicted. It is clear that pitches ranging from a few molecular lengths to a few hundreds of molecular lengths can be reproduced with our theory.

The quantitative merits of the present theory can only be assessed by comparison with experiment for specific values of the interaction parameters of our model. The most important one is the chirality parameter ϵ_c which captures the intrinsic strength of the chiral interactions. Apart from the shape of the mesogen, it is determined primarily by the nature of the long-range electrostatic interactions and the intricate surface structure of the particles; in the case of viruses, for example, the chiral interaction will depend on the helical configuration of surface charges. A change in temperature may induce conformational changes in the chiral structure which affect the magnitude or sign of the pitch. For example, a pitch inversion involving a sudden change of handedness of the cholesteric structure with temperature is known to occur in thermotropic systems[7,95]. These issues are clearly beyond the scope of our coarse-grained model and require a much more detailed representation of the molecular architecture of the mesogen[28,96].

VI.   CONCLUSIONS

An asymptotic analysis of the deformation free energy associated with a cholesteric phase of chiral spherocylinders is presented in this work. The rods consist of a hard spherocylindrical backbone with additional long-ranged achiral (attractive/soft repulsive) and chiral interactions, both represented by a simple square-well form with a range comparable to the length of the rod. Analytical expressions for the twist elastic constant and cholesteric pitch are deduced by invoking a Gaussian approximation for the orientational distribution around the local nematic director. The approach is expected to provide an accurate representation of weakly twisted cholesteric states with a high degree of local nematic ordering which is essentially unaffected by the weak spatial variation of the director field.

The results are relevant to both thermotropic mesogens (e.g., derivatives of cholesterol) and more particularly lyotropic cholesteric systems such as fd virus rods where chiral interactions are mediated predominantly by long-range electrostatic forces[16]. The theory captures the behavior of the cholesteric pitch of fd rods, in particular its non-monotonic variation with temperature and density, as well as the influence of the viral contour length (the effective aspect ratio). An extension of the theory to simple hard-sphere chain models (e.g., see Ref. 97) would enable one to examine the effect of flexibility in more detail.

For attractive SW rods, a steep increase of the pitch is found upon lowering the temperature, in line with experimental observations in thermotropic systems. The steep unwinding of the pitch at low temperatures or high packing fractions is primarily due to a sharp increase of the local nematic order. The prevailing near-parallel rod configurations lead to an anomalous increase of the twist elastic resistance. This simple mean-field scenario contrasts with the commonly expounded view in which the unwinding of the cholesteric is attributed to pre-smectic fluctuations which are geometrically incompatible with a helical structure.

In the future, we plan to validate our theoretical findings with a simulation study of the current chiral spherocylinder model along the lines of Refs. 93,98,99. This will allow us to test the accuracy of the Onsager-Parsons theory in predicting derivative properties such as the elastic constants of dense nematic systems. The simulations would also provide a better insight into the behavior of the cholesteric pitch close to a cholesteric-smectic transition. Finally, it would be intriguing to study the implications of the chiral interactions on the micro-structure of the smectic phase.

Appendix A: Parametrization of the excluded volume of the spherocylinder

The excluded volume manifold of two hard spherocylinders at fixed angle γ is a *spheroparallelepiped* (see Fig. 6) which is most conveniently parametrized by switching from the laboratory frame to a particle frame based on the orientational unit vectors $\hat{\mathbf{u}}_i$. Let us further

define the unit vectors

$$\begin{aligned}
\hat{\mathbf{v}} &= \frac{\hat{\mathbf{u}}_1 \times \hat{\mathbf{u}}_2}{|\sin\gamma|} \\
\hat{\mathbf{w}}_i &= \hat{\mathbf{u}}_i \times \hat{\mathbf{v}}, \quad (i = 1, 2)
\end{aligned} \tag{58}$$

so that $\{\hat{\mathbf{u}}_i, \hat{\mathbf{v}}, \hat{\mathbf{w}}_i\}$ are two orthonormal basis sets in 3D. The centre-of-mass distance vector can be uniquely decomposed in terms of these basis vectors:

$$\mathbf{r}_{12} = (\mathbf{r}_{12} \cdot \hat{\mathbf{u}}_i)\hat{\mathbf{u}}_i + (\mathbf{r}_{12} \cdot \hat{\mathbf{v}})\hat{\mathbf{v}} + (\mathbf{r}_{12} \cdot \hat{\mathbf{w}}_i)\hat{\mathbf{w}}_i. \quad (i = 1, 2) \tag{59}$$

The leading order contribution to the excluded-volume body is of $\mathcal{O}(L^2 D)$ and stems from the overlap of the cylindrical parts of the spherocylinders. This gives rise to a 3D parallelepiped (central section in Fig. 6) which can be parametrized as

$$\mathbf{r}_{12}^{CC} = \frac{L}{2}t_1\hat{\mathbf{u}}_1 + \frac{L}{2}t_2\hat{\mathbf{u}}_2 + Dt_3\hat{\mathbf{v}}, \tag{60}$$

with $-1 \le t_i \le 1$ for $i = 1, 2, 3$. The Jacobian associated with the coordinate transformation is $J_{CC} = \frac{1}{4}L^2 D |\sin\gamma|$. Higher order contributions account for end-cap effects due to the finite thickness of the rods[100]. The first correction term is of $\mathcal{O}(LD^2)$ and originates from an overlap of the hemispherical end-cap of one rod with the cylindrical part of the other. The resulting half cylinders on the four edges of the parallelepiped, at the boundaries of the excluded volume in Fig. 6, can be parametrized as follows:

$$\begin{aligned}
\mathbf{r}_{12}^{CH\pm} &= \mp\frac{L}{2}\hat{\mathbf{u}}_2 + \frac{L}{2}t_1\hat{\mathbf{u}}_1 + t_2 D(\pm\hat{\mathbf{w}}_1\cos\beta + \hat{\mathbf{v}}\sin\beta) \\
\mathbf{r}_{12}^{HC\pm} &= \pm\frac{L}{2}\hat{\mathbf{u}}_1 + \frac{L}{2}t_1\hat{\mathbf{u}}_2 + t_2 D(\pm\hat{\mathbf{w}}_2\cos\beta + \hat{\mathbf{v}}\sin\beta),
\end{aligned} \tag{61}$$

with boundaries $-1 \le t_1 \le 1$, $0 \le t_2 \le 1$ and $\pi/2 \le \beta \le \pi/2$ and Jacobian $J_{CH(HC)\pm} = \frac{1}{2}LD^2 t_2$. The final contribution stems from the spherical segments located at the four corners of the parallelepiped (yellow sections in Fig. 6). These arise from the overlap of two hemispherical end-caps and are of $\mathcal{O}(D^3)$. The segments can be parametrized by invoking a different orthonormal set $\{\hat{\mathbf{u}}_+, \hat{\mathbf{u}}_-, \hat{\mathbf{v}}\}$ where

$$\mathbf{u}_\pm = \hat{\mathbf{u}}_1 \pm \hat{\mathbf{u}}_2, \quad \hat{\mathbf{u}}_\pm = \frac{\mathbf{u}_\pm}{|\mathbf{u}_\pm|}, \tag{62}$$

which leads to the following expression for the centre-of-mass distance corresponding to the four segments:

$$\begin{aligned}
\mathbf{r}_{12}^{HH+\pm} &= \pm\frac{L}{2}\mathbf{u}_+ + rD(\cos\theta\hat{\mathbf{v}} + \sin\theta\sin\varphi_+\hat{\mathbf{u}}_- \\
&\quad \pm \sin\theta\cos\varphi_-\hat{\mathbf{u}}_+) \\
\mathbf{r}_{12}^{HH-\pm} &= \pm\frac{L}{2}\mathbf{u}_- + rD(\cos\theta\hat{\mathbf{v}} + \sin\theta\sin\varphi_-\hat{\mathbf{u}}_+ \\
&\quad \pm \sin\theta\cos\varphi_+\hat{\mathbf{u}}_-),
\end{aligned} \tag{63}$$

with parameter intervals $0 \le r \le 1$, $0 \le \theta \le \pi$, $(\gamma - \pi)/2 \le \varphi_+ \le (\pi - \gamma)/2$ and $-\gamma/2 \le \varphi_- \le \gamma/2$. The
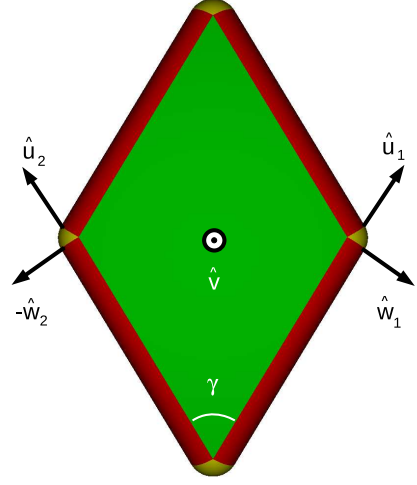

FIG. 6: (Color online). Illustration of the excluded volume manifold of two spherocylinders for a relative orientation angle γ and the unit vectors defined in Eq. (58). The cylinder-cylinder CC, cylinder-hemisphere CH, and hemisphere-hemisphere HH volumetric sections are indicated in green, red and yellow, respectively.

Jacobian associated with the coordinate transformation is $J_{(HH+\pm)(HH-\pm)} = D^3 r^2 \sin\theta$.

For the twist elastic modulus we require the second-moment excluded volume [cf. Eq. (29)]:

$$v_{M_2}(\hat{\mathbf{u}}_1, \hat{\mathbf{u}}_2) = \int_{v_{\text{excl}}} d\mathbf{r}_{12}(\hat{\mathbf{z}} \cdot \mathbf{r}_{12})^2, \tag{64}$$

which can be evaluated separately for each of the excluded volume sections using the parametrization above. The integrations over the parametrization variables can be worked out without difficulty. Let us define the following dot products

$$\begin{aligned}
A_i &= (L/2)\hat{\mathbf{u}}_i \cdot \hat{\mathbf{z}} \\
B &= D\hat{\mathbf{v}} \cdot \hat{\mathbf{z}} \\
C_i &= D\hat{\mathbf{w}}_i \cdot \hat{\mathbf{z}} \\
E_\pm &= D\hat{\mathbf{u}}_\pm \cdot \hat{\mathbf{z}}.
\end{aligned} \tag{65}$$

The cylinder-cylinder CC contribution then reads

$$\begin{aligned}
v_{M_2}^{CC} &= \frac{1}{4}L^2 D |\sin\gamma| \int_{-1}^{1} dt_1 \int_{-1}^{1} dt_2 \int_{-1}^{1} dt_3 (\hat{\mathbf{z}} \cdot \mathbf{r}_{CC})^2 \\
&= \frac{2}{3}L^2 D |\sin\gamma|(A_1^2 + A_2^2 + B^2).
\end{aligned} \tag{66}$$

For the cylinder-hemisphere CH contributions we obtain:

$$
\begin{aligned}
v_{M_2}^{CH} &= \frac{1}{2}LD^2 \int_{-1}^{1} dt_1 \int_{0}^{1} t_2 dt_2 \int_{-\pi/2}^{\pi/2} d\beta \\
&\quad \times \left\{ (\hat{\mathbf{z}} \cdot \mathbf{r}_{CH_+})^2 + (\hat{\mathbf{z}} \cdot \mathbf{r}_{CH_-})^2 + \cdots \right\} \\
&= LD^2 \left\{ \frac{16}{3}(A_1 C_2 - A_2 C_1) + \frac{8\pi}{3}(A_1^2 + A_2^2) \right. \\
&\quad \left. + \pi B^2 + \frac{\pi}{2}(C_1^2 + C_2^2) \right\}.
\end{aligned}
\tag{67}
$$

Finally, for the hemisphere-hemisphere HH contributions we have:

$$
\begin{aligned}
v_{M_2}^{HH} &= D^3 \int_{0}^{1} dr\, r^2 \int_{0}^{\pi} d\theta \sin\theta \\
&\quad \times \left[\int_{(\gamma-\pi)/2}^{(\pi-\gamma)/2} d\varphi_+ \left\{ (\hat{\mathbf{z}} \cdot \mathbf{r}_{HH_{++}})^2 + \cdots \right\} \right. \\
&\quad \left. + \int_{-\gamma/2}^{\gamma/2} d\varphi_- \left\{ (\hat{\mathbf{z}} \cdot \mathbf{r}_{HH_{-+}})^2 + \cdots \right\} \right] \\
&= D^3 \left\{ \frac{4}{3}\gamma(E_- |\mathbf{u}_-|)^2 + \frac{4}{3}(\pi-\gamma)(E_+ |\mathbf{u}_+|)^2 \right. \\
&\quad + \frac{4\pi}{15}(E_+^2 + E_-^2 + B^2) \\
&\quad \left. + \pi\left(|\mathbf{u}_+| E_+^2 \cos\frac{\gamma}{2} + |\mathbf{u}_-| E_-^2 \sin\frac{\gamma}{2} \right) \right\}.
\end{aligned}
\tag{68}
$$

It is easily verified that all contributions are symmetric under inversion $\hat{\mathbf{u}}_i \to -\hat{\mathbf{u}}_i$ and interchanging $\hat{\mathbf{u}}_1 \leftrightarrow \hat{\mathbf{u}}_2$, as required. The total expression Eq. (64) is obtained by adding the contributions from the different sections, $v_{M_2} = v_{M_2}^{CC} + v_{M_2}^{CH} + v_{M_2}^{HH}$, which provides an analytic result for the moment excluded volume of two spherocylinders of arbitrary aspect ratio.

For the twist energy one requires the first-moment excluded volume over the pseudo-scalar T_{212}. Recalling Eq. (15) we get

$$
v_{M_1}(\hat{\mathbf{u}}_1, \hat{\mathbf{u}}_2) = \cos\gamma \int_{v_{excl}} d\mathbf{r}_{12} (\hat{\mathbf{z}} \cdot \mathbf{r}_{12})(\hat{\mathbf{u}}_1 \times \hat{\mathbf{u}}_2 \cdot \hat{r}_{12}), \tag{69}
$$

with $\cos\gamma = \hat{\mathbf{u}}_1 \cdot \hat{\mathbf{u}}_2$. Exploiting the orthogonality of the unit vectors and collecting terms gives for the leading order contribution:

$$
v_{M_1}^{CC} = \frac{1}{4}L^2 DB \sin^2\gamma \cos\gamma \, \mathcal{F}_{CC}(x, \gamma). \tag{70}
$$

Here, $\mathcal{F}_{CC}$ represents a triple integral:

$$
\mathcal{F}_{CC}(x, \gamma) = \prod_{i=1}^{3} \int_{-1}^{1} dt_i \frac{t_3^2}{\sqrt{\frac{t_1^2}{4x^2} + \frac{t_2^2}{4x^2} + t_3^2 + \frac{2t_1 t_2}{4x^2} \cos\gamma}}, \tag{71}
$$

which cannot be solved in closed form. In the asymptotic limit ($\cos\gamma \sim 1$) $\mathcal{F}_{CC}$ becomes a function of the inverse aspect ratio $x = D/L$ only, and no longer plays a role in the subsequent angular averaging. It is enlightening to expand the argument as a Taylor series:

$$
\frac{t_3^2}{\sqrt{\frac{t_1^2}{4x^2} + \frac{t_2^2}{4x^2} + t_3^2 + \frac{2t_1 t_2}{4x^2}}} = \frac{2t_3^2}{|t_1 + t_2|}x + \mathcal{O}(x^3), \tag{72}
$$

from which one finds that the leading order CC contribution is of $\mathcal{O}(LD^3)$ and thus of marginal importance for the relevant range of aspect ratios $L/D > 10$. The integration over the CH parts requires more effort, but the result can be cast in a similar form:

$$
v_{M_1}^{CH} = \frac{1}{2}LD^2 B |\sin\gamma| \cos\gamma \, \mathcal{F}_{CH}(x, \gamma), \tag{73}
$$

with

$$
\mathcal{F}_{CH}(x, \gamma) = \int_{-1}^{1} dt_1 \int_{0}^{1} dt_2 t_2 \int_{-\pi/2}^{\pi/2} d\beta \sum_{\pm} \frac{2t_2^2 \sin^2\beta}{r_{12}^{CH\pm}}. \tag{74}
$$

Here, $r_{12}^{CH\pm}$ represents the vector norms:

$$
r_{12}^{CH\pm} = \sqrt{\frac{1}{4x^2} + \frac{t_1^2}{4x^2} + t_2^2 \pm \frac{t_1}{2x^2} + \frac{t_2}{2x}\cos\beta |\sin\gamma|}. \tag{75}
$$

Without further analyzing $\mathcal{F}_{CH}$ it is evident that the CH contributions are small and at least of $\mathcal{O}(LD^3)$. The HH integrations will produce terms of even higher order in D and therefore the analysis need not be pursued any further.

Appendix B: Gaussian averages

The Gaussian averages required for the evaluation of H_0 and H_2 [Eq. (42) and Eq. (44)] have been deduced by Odijk[88]. We quote them here:

$$
\begin{aligned}
\langle\langle |\gamma| \theta_1^2 (\theta_1^2 + \theta_2^2) \rangle\rangle &\sim \frac{35}{2}\pi^{1/2}\alpha^{-5/2} \\
\langle\langle |\gamma|^3 \theta_1^2 \rangle\rangle &\sim 21\pi^{1/2}\alpha^{-5/2} \\
\langle\langle |\gamma|^3 \rangle\rangle &\sim 6\pi^{1/2}\alpha^{-3/2} \\
\langle\langle |\gamma| \theta_1^2 \rangle\rangle &\sim \frac{5}{2}\pi^{1/2}\alpha^{-3/2}.
\end{aligned}
\tag{76}
$$

The last term in Eq. (44) can be evaluated in two steps. Since $\theta_1^2(\theta_2^2 - \theta_1^2)/|\gamma| \sim \mathcal{O}(\theta^3)$ a simple Gaussian integral suffices to establish the following scaling result:

$$
\left\langle \left\langle \frac{\theta_1^2(\theta_2^2 - \theta_1^2)}{|\gamma|} \right\rangle \right\rangle \propto \alpha \int_{0}^{\infty} d\theta \theta^4 \exp\left[-\frac{\alpha\theta^2}{2} \right] \sim p\alpha^{-3/2}. \tag{77}
$$

The pre-factor p is obtained by numerical evaluation of the following triple integral:

$$
\begin{aligned}
p &= \alpha^{7/2} \int_{0}^{\pi/2} d\theta_1 \theta_1 \int_{0}^{\pi/2} d\theta_2 \theta_2 \int_{0}^{2\pi} \frac{d\Delta\varphi}{2\pi} \\
&\quad \times \exp\left[-\frac{\alpha}{2}(\theta_1^2 + \theta_1^2) \right] \frac{\theta_1^2(\theta_2^2 - \theta_1^2)}{|\gamma|},
\end{aligned}
\tag{78}
$$

which gives $p = -1.772$ for any given $\alpha \gg 1$.

Acknowledgments

[*] Electronic address: r.wensink@imperial.ac.uk

[1] P. G. de Gennes and J. Prost, *The Physics of Liquid Crystals* (Clarendon Press, Oxford, 1993).

[2] F. Reinitzer, Monatsh. Chem. **9**, 421 (1888).

[3] O. Z. Lehmann, Phys. Chem. (Leipzig) **4**, 462 (1889).

[4] C. Robinson, Tetrahedron **13**, 219 (1961).

[5] F. Livolant and A. Leforestier, Prog. Polym. Sci. **21**, 1115 (1996).

[6] Z. Dogic and S. Fraden, Curr. Opin. Colloid Interface Sci. **11**, 47 (2005).

[7] I. Uematsu and Y. Uematsu, Adv. Pol. Sci. **59**, 37 (1984).

[8] D. B. DuPré and E. T. Samulski, in *Liquid Crystals: the Fourth State of Matter*, edited by F. D. Saeva (Dekker, New York, 1979).

[9] T. Sato and A. Teramoto, Adv. Polym. Sci. **126**, 85 (1996).

[10] R. S. Werbowyj and D. G. Gray, Mol. Cryst. Liquid Cryst. **34**, 97 (1976).

[11] K. Hiltrop, in *Chirality in Liquid Crystals*, edited by H. S. Kitzerow and C. Bahr (Springer-Verlag, New York, 2001).

[12] D. H. Vanwinke, M. W. Davidson, W. X. Chen, and R. L. Rill, Macromolecules **23**, 4140 (1990).

[13] Y. M. Yevdokimov, S. G. Skuridin, and V. I. Salyanov, Liq. Cryst. **11**, 1443 (1988).

[14] C. B. Stanley, H. Hong, and H. H. Strey, Biophys. J. **89**, 2552 (2005).

[15] Z. Dogic and S. Fraden, Langmuir **16**, 7820 (2000).

[16] E. Grelet and S. Fraden, Phys. Rev. Lett. **90**, 198302 (2003).

[17] D. B. DuPré and R. W. Duke, J. Chem. Phys. **63**, 143 (1975).

[18] K. Yoshiba, A. Teramoto, N. Nakamura, and T. Sato, Macromolecules **36**, 2108 (2003).

[19] X. M. Dong and D. G. Gray, Langmuir **13**, 2404 (1997).

[20] A. F. Miller and A. M. Donald, Biomacromolecules **4**, 510 (2003).

[21] X. M. Dong, T. Kimura, J. F. Revol, and D. G. Gray, Langmuir **12**, 2076 (1996).

[22] T. Sato, Y. Sato, Y. Umemura, A. Teramoto, Y. Nagamura, J. Wagner, D. Weng, Y. Okamoto, K. Hatada, and M. M. Green, Macromolecules **26**, 4551 (1993).

[23] A. B. Harris, R. D. Kamien, and T. C. Lubensky, Rev. Mod. Phys. **71**, 1745 (1999).

[24] H. H. Strey, R. Podgornik, D. C. Rau, and V. A. Parsegian, Curr. Opin. Struct. Biol. **3**, 534 (1998).

[25] A. A. Kornyshev and S. Leikin, J. Chem. Phys. **107**, 7035 (E) (1997).

[26] A. A. Kornyshev and S. Leikin, Phys. Rev. Lett. **84**, 2537 (2000).

[27] A. A. Kornyshev, S. Leikin, and S. V. Malinin, Eur. Phys. J. E **7**, 83 (2002).

[28] F. Tombolato and A. Ferrarini, J. Chem. Phys. **122**, 054908 (2005).

[29] W. J. A. Goossens, Mol. Cryst. Liq. Cryst. **12**, 237 (1971).

[30] B. W. van der Meer and G. Vertogen, in *The Molecular Physics of Liquid Crystals*, edited by G. R. Luckhurst and G. W. Gray (Academic Press, New York, 1979).

[31] B. W. van der Meer, G. Vertogen, A. J. Dekker, and J. G. J. Ypma, J. Chem. Phys. **65**, 2580 (1976).

[32] Y. R. Lin-Liu, Y. M. Shih, and C. W. Woo, Phys. Rev. A **15**, 2550 (1977).

[33] L. Hu, Y. Jiang, T. D. Lee, and R. Tao, Phys. Rev. E **57**, 4289 (1998).

[34] M. A. Osipov and H.-G. Kuball, Eur. Phys. J. E **5**, 589 (2001).

[35] A. Kapanowski, Z. Naturforsch. **57A**, 105 (2002).

[36] A. V. Emelyanenko, Phys. Rev. E **67**, 031704 (2003).

[37] L. Onsager, Ann. N.Y. Acad. Sci. **51**, 627 (1949).

[38] S. Varga and G. Jackson, Mol. Phys. **104**, 3681 (2006).

[39] J. P. Straley, Phys. Rev. A **14**, 1835 (1976).

[40] T. Odijk, J. Phys. Chem. **91**, 6060 (1987).

[41] R. A. Pelcovits, Liq. Cryst. **21**, 361 (1996).

[42] A. Saupe, Z. Naturforsch. **15A**, 810; *ibid.* 815 (1960).

[43] J. Nehring and A. Saupe, J. Chem. Phys. **56**, 5527 (1972).

[44] B. W. van der Meer, Phys. Lett. A **59**, 279 (1976).

[45] R. G. Priest, Phys. Rev. A **7**, 720 (1973).

[46] J. P. Straley, Phys. Rev. A **8**, 2181 (1973).

[47] A. Poniewierski and J. Stecki, Mol. Phys. **38**, 1931 (1979).

[48] S. D. Lee, Phys. Rev. A **39**, 3631 (1989).

[49] J. Stecki and A. Poniewierski, Mol. Phys. **41**, 1451 (1980).

[50] W. M. Gelbart and A. Ben-Shaul, J. Chem. Phys. **77**, 916 (1982).

[51] G. Vertogen and W. H. de Jeu, *Thermotropic Liquid Crystals, Fundamentals* (Springer Ser. Chem. Phys., Berlin, 1988).

[52] H. Steuer and S. Hess, Phys. Rev. Lett. **94**, 027802 (2005).

[53] B. W. van der Meer, F. Postma, A. J. Dekker, and W. H. de Jeu, Mol. Phys. **45**, 1227 (1982).

[54] E. Govers and G. Vertogen, Liq. Cryst. **2**, 31 (1987).

[55] D. Coates and G. W. Gray, Mol. Cryst. Liq. Cryst. **24**, 163 (1973).

[56] S. Tomar, M. M. Green, and L. A. Day, J. Am. Chem. Soc. **129**, 3367 (2007).

[57] F. Tombolato, A. Ferrarini, and E. Grelet, Phys. Rev. E **96**, 258302 (2006).

[58] R. Alben, Mol. Cryst. Liq. Cryst. **20**, 231 (1973).

[59] R. S. Pindak, C. C. Hang, and J. T. Ho, Phys. Rev. Lett. **32**, 43 (1974).

[60] T. Harada and P. Crooker, Mol. Cryst. Liq. Cryst. **30**, 79 (1975).

[61] G. Durand, Comptes Rendus Acad. Sci. **B264**, 1251 (1967).

[62] J. Watanabe and T. Nagase, Macromolecules **21**, 171 (1988).

[63] T. Yamagishi, T. Fukada, T. Miyamoto, T. Ichizuka, and J. Watanabe, Liq. Cryst. **7**, 155 (1990).

[64] E. Sackmann, S. Meiboom, L. C. Snyder, A. E. Meixner, and R. E. Dietz, J. Am. Chem. Soc. **90**, 3567 (1968).

[65] F. Livolant, A. M. Levelut, J. Doucet, and J. P. Benoit, Nature **339**, 724 (1989).

[66] H. Kimura, M. Hosino, and H. Nakano, J. Phys. Soc. Jpn **51**, 1584 (1982).

[67] J. Saha and M. Saha, Mol. Sim. **19**, 227 (1997).

[68] M. P. Allen, G. T. Evans, D. Frenkel, and B. M. Mulder, Adv. Chem. Phys. **86**, 1 (1993).

[69] F. C. Frank, Discuss. Faraday Soc. **25**, 19 (1958).

[70] T. Odijk and H. N. W. Lekkerkerker, J. Phys. Chem. **89**, 2090 (1985).

[71] A. Gil-Villegas, S. C. McGrother, and G. Jackson, Chem. Phys. Lett. **269**, 441 (1997).

[72] A. Gil-Villegas, S. C. McGrother, and G. Jackson, Mol. Phys. **92**, 723 (1997).

[73] S. C. McGrother, A. Gil-Villegas, and G. Jackson, Mol. Phys. **95**, 657 (1998).

[74] S. C. McGrother, A. Gil-Villegas, and G. Jackson, J. Phys.:Condens. Matter **8**, 9649 (1996).

[75] W. M. Gelbart and B. A. Baron, J. Chem. Phys. **66**, 207 (1977).

[76] M. Franco-Melgar, Ph.D. thesis, Imperial College London (2006).

[77] M. Franco-Melgar, A. J. Haslam, and G. Jackson, Mol. Phys. **106**, 649 (2008).

[78] J. D. Parsons, Phys. Rev. A **19**, 1225 (1979).

[79] S. D. Lee, J. Chem. Phys. **87**, 4972 (1987).

[80] S. D. Lee, J. Chem. Phys. **89**, 7036 (1989).

[81] N. F. Carnahan and K. E. Starling, J. Chem. Phys. **51**, 635 (1969).

[82] J. P. Hansen and I. R. McDonald, *Theory of Simple Liquids* (Academic Press, New York, 2006).

[83] G. Jackson, J. S. Rowlinson, and C. A. Leng, J. Chem. Soc., Faraday Trans. 1 **82**, 3461 (1986).

[84] D. G. Green and G. Jackson, J. Chem. Phys. **97**, 8672 (1992).

[85] A. L. Archer, M. D. Amos, G. Jackson, and I. A. McLure, Int. J. Thermophys. **17**, 201 (1996).

[86] A. Galindo, P. J. Whitehead, G. Jackson, and A. N. Burgess, J. Phys. Chem. **100**, 6781 (1996).

[87] M. N. Garcia-Lisbona, A. Galindo, G. Jackson, and A. N. Burgess, J. Am. Chem. Soc. **120**, 4191 (1998).

[88] T. Odijk, Liq. Cryst. **1**, 553 (1986).

[89] G. J. Vroege and H. N. W. Lekkerkerker, Rep. Prog. Phys. **55**, 1241 (1992).

[90] R. Alben, J. Chem. Phys. **59**, 4299 (1973).

[91] S. C. McGrother, D. C. Williamson, and G. Jackson, J. Chem. Phys. **104**, 6755 (1996).

[92] P. Bolhuis and D. Frenkel, J. Chem. Phys. **106**, 666 (1997).

[93] S. Varga and G. Jackson, Chem. Phys. Lett. **377**, 6 (2003).

[94] P. G. de Gennes, Mol. Cryst. Liq. Cryst. **21**, 49 (1973).

[95] A. Sikora, T. A. Siromyatnikova, B. M. Ginzburg, Y. A. Alumyan, A. A. Shepelevskii, and S. Y. Frenkel, Makromol. Chem. **189**, 201 (1988).

[96] A. A. Kornyshev and S. Leikin, J. Chem. Phys. **107**, 3656 (1997).

[97] D. C. Williamson and G. Jackson, J. Chem. Phys. **108**, 10294 (1998).

[98] M. P. Allen and A. J. Masters, Mol. Phys. **79**, 277 (1993).

[99] B. T. Tjipto-Margo, G. T. Evans, M. P. Allen, and D. Frenkel, J. Phys. Chem. **96**, 3942 (1992).

[100] R. van Roij, Ph.D. thesis, Utrecht University (1996).